DEVELOPMENT OF A LINE LIST FOR AUTOMATION OF STELLAR ABUNDANCE ANALYSIS

A Thesis
by
DAVID GRIBBLE

Submitted to the Graduate School
at Appalachian State University
in partial fulfillment of the requirements for the degree of
MASTER OF SCIENCE

August 2018
Department of Physics and Astronomy

DEVELOPMENT OF A LINE LIST FOR AUTOMATION OF STELLAR ABUNDANCE ANALYSIS

A Thesis
by
DAVID GRIBBLE
August 2018

APPROVED BY:

Michael Briley, Ph.D.
Chairperson, Thesis Committee

Richard Gray, Ph.D.
Member, Thesis Committee

Courtney McGahee, Ph.D.
Member, Thesis Committee

Michael Briley, Ph.D.
Chairperson, Department of Physics and Astronomy

Michael J. McKenzie, Ph.D.
Dean, Cratis D. Williams School of Graduate Studies

Abstract

DEVELOPMENT OF A LINE LIST FOR AUTOMATION OF STELLAR ABUNDANCE ANALYSIS

David Gribble
B.S., University of California, Davis
M.S., Appalachian State University

Chairperson: Michael Briley, Ph.D.

Studies of abundances in stars have a wide range of application to many topics in stellar, galactic, and nuclear astrophysics. By looking at abundances of elements in stars and clusters, we can draw conclusions about the histories of those clusters and of the stars within them. And by looking at stars that may not match our current theories of stellar evolution, we can close some of the gaps in our understanding of the evolution and lifecycles of stars. As surveys get increasingly larger and generate progressively more data, having tools that facilitate the automatic processing of these large data sets becomes ever more desirable.

In this paper, we develop a "line list" of 428 transitions necessary for detailed abundance analyses of high-resolution spectra, and then present a semi-automated method for determining abundances from equivalent width measurements through the use of the line list with the spectral-line fitting software DAOSpec, the MARCS grid of model atmospheres, and the spectral-line analysis software MOOG. We demonstrate our line list and abundance analysis tools on two different stars, NGC 6940 101 and IC 4756 14. We present our derived stellar atmosphere parameters for those stars and give detailed abundance analyses. We then

compare these results to those found in other studies to demonstrate the quality and reliability of our tools.

Acknowledgments

This work was made possible with funding and support from NASA/North Carolina Space Grant and with observations taken at McDonald Observatory. The author would like to thank Peter Stetson, for helpful correspondences and code suggestions, and Michael Briley for contributing observational data, and contributing the section in Chapter 2.1 describing those observations. The author expresses his gratitude to Michael Briley, Richard Gray, and Courtney McGahee for their support as well as their insightful comments and suggestions for improving the paper. This research made use of the IRAF, DAOSpec, MOOG, and MARCS software packages.

Dedication

To all of the scientists who have inspired, supported, and encouraged me over the years, without whom, I would not be where I am today. People who give unconditionally, with no expectation of a return, simply because they sincerely care about the next generation of scientists. I hope to be able to pay those gifts forward in some way. Ron Mickens, Tom Cahill, Charles Ferguson, Sid Clements, Patricia Boeshaar. To Edward Bouchet. To Bryce Case Jr. And to Henry Mosely.

Table of Contents

Chapter 1. Introduction

Studies of abundances in stars have a wide range of application to many topics in stellar, galactic, and nuclear astrophysics. By looking at abundances of elements in stars and clusters, we can draw conclusions about the histories of those clusters and of the stars within them. Broadly, this research is concerned with closing the gaps in our understanding of the evolution and lifecycles of stars by looking at stars that may not match our current theories of stellar evolution.

As surveys become increasingly larger and generate progressively more data, having tools that facilitate the automatic processing of these large data sets becomes ever more desirable. In this paper, we develop a "line list" — a reference list of atomic transitions corresponding to various absorption lines, and the excitation potentials and transition probabilities associated with those transitions — necessary for detailed abundance analyses, and then present a semi-automated method for determining abundances from equivalent width measurements through the use of the line list with multiple software packages. Through this process, we also set up tools useful to accommodate the processing of other large spectroscopic data sets.

We test our line list and abundance analysis tools on two different program stars, NGC 6940 101 and IC 4756 14. We present our derived stellar atmosphere parameters for those stars and give detailed abundance analyses. We then compare these results to those found in other studies to demonstrate the quality and reliability of our tools.

We use observations taken with the high-resolution spectrograph on the 2.7-meter telescope at the McDonald Observatory, and apply the automated spectral-line fitting

software DAOSpec (Stetson & Pancino 2008) to these large data sets. We then run a well-known star such as the Sun through the software to identify and measure the equivalent widths of several hundreds of lines. Using a star with a well-known chemical composition allows us to deduce the atomic parameters for the spectral-lines using appropriate stellar atmospheres from the MARCS grid of model atmospheres (Gustafsson et al. 1975) and modeling tools from MOOG (Sneden 1973). Once developed, we in turn apply the line list to stars with unknown compositions to produce detailed abundance analyses and atmospheric parameters.

We describe the structure of the rest of the paper as follows. In Chapter 2, we explain the reasoning and scientific basis behind our methods. We describe some of the fundamental scientific background behind abundance research, and explain some of the motivation to pursue this kind of inquiry. We explain some useful terms and concepts, and then discuss traditional approaches to abundance analyses and how this study fits into those. We end the chapter by summarizing some of the current research topics for which abundance analyses are important, and then give a brief overview of the various notations used in the field to describe elemental abundances, which may be unfamiliar to readers not already engaged in abundance research.

In Chapter 3, we describe the construction and assembly of our line list, our method for how to prepare spectra for use with the line list, and how to use the line list to analyze stellar spectra. We describe our observations, and then give a brief overview of the various software packages referred to in this study, before finally supplying a detailed summary of the rectification process of the spectra and of the development and use of the line list.

In Chapter 4, we give the results of our abundance analyses and then discuss them in the context of previous studies. We list our derived atmospheric parameters of effective temperature, surface gravity, and microturbulence for our two program stars, followed by their respective abundances. We then compare these parameters and abundances with those previously found in the literature. We find that our results agree with previous studies. Finally, we discuss potential areas for improvement of our tools and highlight topics for further study.

Chapter 2. Justification and Literature Review

Typically, researchers doing abundance analyses would have to painstakingly measure each line in a spectrum by hand. This is a very time-consuming process, and a researcher could spend the majority of their time measuring and identifying hundreds of lines by hand. As a result, some studies may choose to only focus on certain elements of interest — such as iron, titanium, chromium, and vanadium — rather than a complete survey of element abundances, or may only look at a very limited band of wavelengths or at a limited subset of lines that represent certain elements, in order to accommodate surveys of multiple stars. By adopting such limitations, researchers may make a tradeoff between statistical significance in number of absorption lines evaluated, and statistical significance in number of stars evaluated in a cluster, e.g. having one star with a detailed abundance analysis vs many similar-type stars in the same cluster with limited/less precise abundance data for each. By automating parts of this analysis, we are creating tools to significantly reduce the amount of time that is spent on equivalent width measurements and which allow for the processing of large spectroscopic data sets. This reduces the necessity of tradeoffs such as the ones mentioned above.

With the methods developed and described in this paper, we expect to obtain and be able to constrain values for stellar atmospheric parameters of effective temperature, surface gravity, and microturbulence, as well as abundance values for a wide range of elements.

2.1 Description of Microturbulence

The term “microturbulence” is used frequently in stellar astrophysics to essentially describe a contribution to spectral-line broadening resulting from turbulent velocities of

atoms in the atmosphere of a star. These turbulent velocities cause absorption lines to be broadened, and if unaccounted for, can make it appear as though the thermal contribution is enhanced (Böhm-Vitense 1989; Gray 2005).

2.2 Description of Instrumental Profile

Another contribution to spectral-line broadening is referred to as the "instrumental profile" of the spectrograph. This is also sometimes alternatively called the "line-spread function." It is a distortion of the spectral-line profile due to the finite resolution of the spectrograph. The instrument then gives a line profile a certain shape, which is especially noticeable for low dispersion spectra (Böhm-Vitense 1989). When convolved with the intrinsic stellar line profile, the result is the observed line profile.

2.3 Importance of Equivalent Widths

We know to first-order that for absorption lines for which the line core is not saturated, equivalent widths are proportional to the number of absorbing atoms times the oscillator strength, and that oscillator strength is proportional to transition probability (Böhm-Vitense 1989). Therefore, if we want to determine the abundance of a specific element present in a star, which we know is related to the number of absorbing atoms in our line of sight, the number of absorbing atoms is proportional to the equivalent width divided by the transition probability. If one knows the temperature of a star, which we determine using a model of the stellar atmosphere, one could then apply the Boltzmann formula here to determine the number of atoms of that element that are present (Böhm-Vitense 1989). Therefore, if we know the atomic transition probabilities, as well as the stellar parameters, then we can use the measurement of equivalent widths of elemental lines of interest to determine the abundances of those elements in a star.

2.4 Summary of Traditional Equivalent Width Method

The Böhm-Vitense text (1989) gives a good summary of the process by which a researcher would determine chemical abundances by hand by measuring equivalent widths and using curve of growth analysis. To determine abundances, one must first "identify" the collection of absorption lines from a star's spectrum that are under consideration. That is, they need to be matched with their corresponding elements and transitions. To do this, the wavelengths of the lines are measured, and then compared to a table of known lines and their corresponding transitions. Our automation of this process, using the DAOSpec software is described in Chapter 3. As in our automated process, there is an uncertainty associated with this wavelength measurement, and thus there are usually about three to four nearby line identification candidates in the table (Böhm-Vitense 1989). It is then necessary to distinguish the most likely candidate among them.

Once identified, the researcher uses the measured equivalent width to find the location of the absorption line in a curve of growth. The curves of growth are essentially log-log plots of line strengths as a function of the number of absorbers (Gray 2005). Typically, a researcher may then have to use the information determined from the curve of growth, with the Boltzmann and Saha equations to determine abundances, ionization ratios, temperature, and gravity (Böhm-Vitense 1989).

2.5 Summary of Alternative Methods

Alternatively, some other researchers may use a spectral synthesis method, that basically works through trial-and-error. In this method, abundance values and relevant model parameters of effective temperature, surface gravity, and microturbulence are used to produce a synthetic stellar spectrum. The abundances and parameters are then adjusted until

a sufficiently accurate version of the observed spectrum is computationally reproduced (Gray 2005). As with the traditional equivalent width measuring method, this is also a very time-consuming process. Despite the time-commitment necessary for producing good results with spectral synthesis, the method can be quite useful for determining abundances for lighter elements and for examining crowded regions, heavily-blended lines, hyperfine structure, and molecular bands. Some examples of this type of spectral synthesis software include SPECTRUM (Gray & Corbally 1994) and ATLAS9 (Kurucz & Avrett 1981). The MOOG software (Sneden 1973), used later in this paper, is also capable of this type of analysis.

2.6 Applications of Abundance Analysis & Relevant Topics

Chemical abundances are of interest for many topics in stellar, galactic, and nuclear astrophysics. Chemical evidence can be used to tell us about the nuclear reactions taking place in stars, as well as about the nuclear reactions that once took place in earlier progenitor stars and supernovae. Since we expect stars that formed at different times and in different places to inherit information concerning the composition of the material from which they formed (Gray 2005), chemical abundances can provide insight into the ways stars evolve and can help us better understand the chemical evolution of our galaxy.

Abundances are especially of interest to researchers studying different stellar populations, e.g. traditional and observable Population I and II stars. Abundances are also important to those trying to better understand the first stars that formed in the universe, known as Population III stars. Searches for ultra metal-poor stars are of interest here, as these earliest stars would have no progenitor stars to enrich them with heavier elements beyond those formed from big-bang nucleosynthesis and are thus theorized to be formed from the available hydrogen, helium, and lithium.

For example, two useful tracers of age and evolutionary stage of a star are lithium and carbon isotope abundances (Gray 2005). Since lithium is destroyed at temperatures approaching 2×10^6 K, and the convection zone of a star brings lithium to the interior layers where it is destroyed as it is converted to helium, lithium can be used to indicate the age of a star. Another exciting source of interest for following lithium abundances in stars, is the observation of some giant stars with unusually large lithium abundances (Gray 2005). Due to their age and deep convection zones, as previously mentioned, these stars should have fused their lithium into helium long ago.

Additionally, abundances can be used to infer information about internal mixing of material in stars, penetration depths of convection zones, diffusion and gravitational settling, and accretion of material from interstellar space (Gray 2005). Some additional topics include chemically peculiar stars, stars with unexplained and anomalous abundances of unusual elements, and stars with large amounts of unidentified lines.

2.7 Notation

As is common in the literature, abundances determined in this paper are reported in the appendices as 12 plus the base-10 logarithm of the number of atoms of the element relative to hydrogen (Gray 2005). This is also the notation used in the output of MOOG. Other common notations include simply the base-10 logarithm of the number of atoms of the element relative to hydrogen (in other words, not normalized to $\log N(\mathrm{H})=12$), and as a logarithmic ratio of an element's abundance in a star relative to that of the Sun (represented as [*N*/H], where $[N/\mathrm{H}] = \log(\mathrm{element/H})_{\mathrm{star}} - \log(\mathrm{element/H})_{\mathrm{Sun}}$). We convert our values to the [*N*/H] notation for the main body of the article, in order to compare with data from other studies.

Chapter 3. Description of Research

3.1 Observations

Program stars were observed on the nights of 1999 August 7 and 8 with the McDonald Observatory's 2.7-meter telescope, cross-dispersed "2D-Coudé" echelle spectrograph (Tull et al. 1995), and a Tektronics 2048x2048 CCD detector (TK3). The cs23 configuration was used resulting in a two-pixel resolution of R = $\lambda/\Delta\lambda$ of 60,000 at 8005 Å. A slit width of 3.5μm (1.2 arc sec) was employed throughout and the seeing varied from 1.0 to 1.5 arc sec. Use of a long slit allowed for sky subtraction, while still maintaining sufficient order separation. Exposures of bright, hot, rapidly rotating stars were made at the start and end of each night to aid in the removal of the telluric lines. Spectra were also taken of the Sun through a frosted glass during day. The program stars themselves were observed with 1800s integrations and multiple observations of the same star were cleaned of cosmic rays by hand, divided by the spectra of the hot stars to minimize telluric absorption features, and averaged. Reduction followed standard procedures using the Image Reduction and Analysis package (IRAF).[1]

3.2 Software Overview

DAOSpec takes an input spectrum, and identifies and measures the equivalent widths (EW) of absorption lines. It then compares these lines to an input reference "line list," based on wavelength, and returns an output with the observed wavelength of the absorption line, the measured EW, and if matched to a wavelength/line in the line list, the corresponding entry (everything included on the line) from the line list. DAOSpec automatically measures

[1] IRAF is distributed by the National Optical Astronomy Observatories, which are operated by the Association of Universities for Research in Astronomy, Inc., under cooperative agreement with the National Science Foundation.

these absorption lines, but it requires a good reference line list in order for those measurements to be useful. Because the lines from the line list are simply appended onto the DAOSpec output, we want the line list to include all information that we would like to attach to a measured line for use with other programs (atomic data for an absorption at that wavelength, such as element, ionization state, etc.).

MOOG uses the line measurement data with corresponding atomic data, and a model atmosphere based on the star to be analyzed, which includes effective temperature, surface gravity, and microturbulence. It uses this information to calculate, and then output, the abundances for each element.

To create an atmosphere model, the Multimoog wrapper takes a set of measured Fe I and Fe II lines with atomic data, and iteratively builds a model atmosphere using MARCS, that can be used with MOOG. It iterates by executing MOOG, using the generated atmosphere model file, then uses those results to modify the model (changes temperature, surface gravity, and microturbulence), and iterates until the MOOG results for the Fe I and Fe II lines are adequately consistent.

One of the difficulties persistent through all this is taking the respective outputs at these different steps, and putting them into a format useable as input to be combined with the other steps, in order to better automate and streamline a procedure that produces meaningful results.

3.3 Methods of Analysis

3.3.1 Preliminary Rectification of Spectra

After observational data was obtained, standard reduction practices were followed, using the IRAF suite. The spectra usually follow a rising continuum, i.e. intensity increases

with increasing wavelength, due to the response of the spectrograph and as an artifact of the diffraction grating. This makes it hard to compare the strength of lines at different wavelengths, so we manipulate them mathematically to normalize — or "rectify" — them to a flat continuum. We used multiple hot stars to fit an instrumental response curve and remove that from the program star spectra. The hot stars used were BS 7040 and BS 7708. This first required finding an equation that fit the spectra of the hot stars, since the atoms in hot stars are mostly ionized due to the high temperatures, and so their spectra are less cluttered by absorption lines. As a result, this means that the precise determination of the location of the continuum is less demanding for these kinds of stars (Gray 2005).

Using the SFIT function in IRAF, we fit a 4^{th} order Legendre polynomial, to match the continuum in each aperture of the hot stars. The fit lines/continua were combined, using the SCOMBINE function in IRAF. In order to normalize our flat continuum, we divided each aperture of the combined fit by a straight line having the mean value of the fit at that aperture. This straight line was created by fitting a 1^{st} order Legendre polynomial with no rejection to the combined fit line. Finally, in order to complete the rectification process, the spectra for each program star (including the Sun) were divided by the previously mentioned "combined average." Comparisons of the spectra before and after rectification are shown in figures 1, 2, and 3. Then, in order to make the rectified spectra useable with other software packages such as DAOSpec, the apertures were separated into individual files in IRAF using the function, SCOPY.

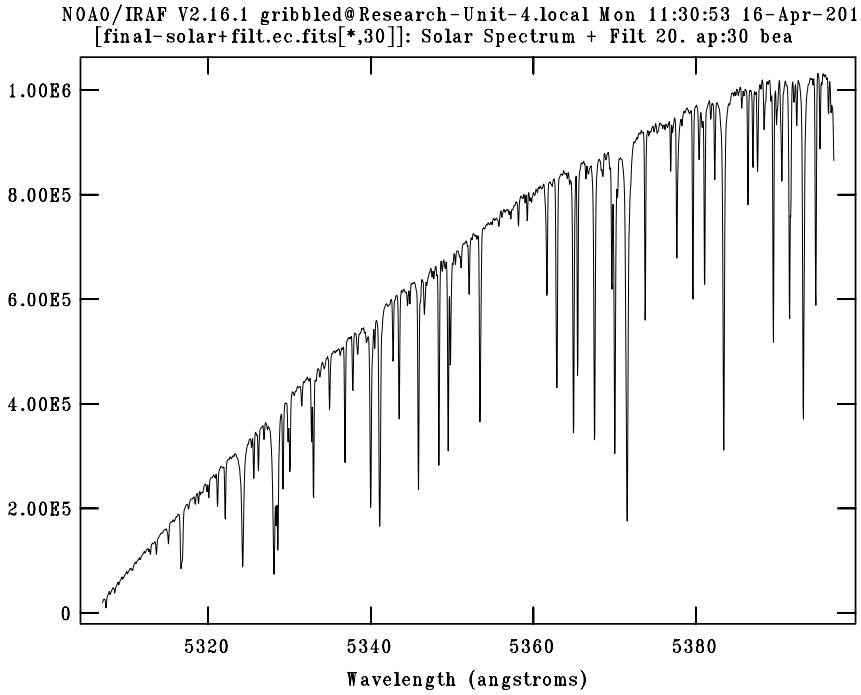

Figure 1: Example of spectra prior to rectification.

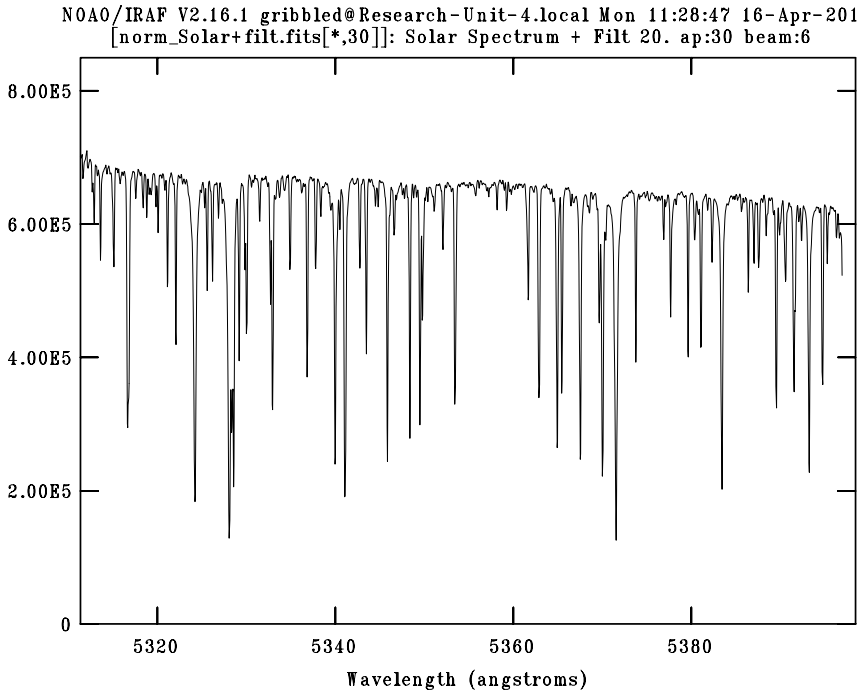

Figure 2: Example of spectra after rectification; note the improved flatness and approximate location of the continuum.

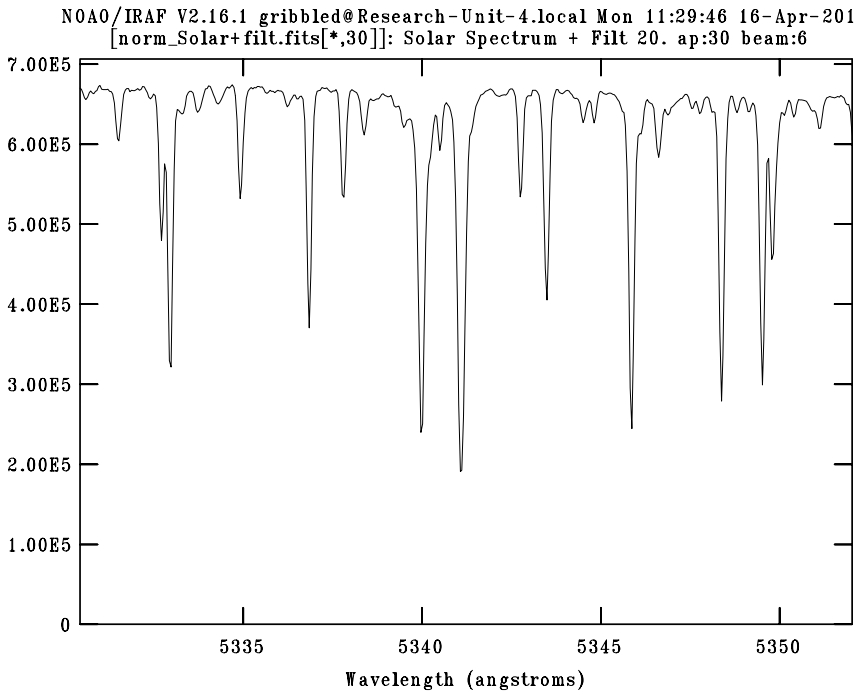

Figure 3: Example of some typical individual lines with continuum visible; shown after rectification.

3.3.2 Development of Line List

In order to build up our line list, after we find and measure equivalent widths of lines with DAOSpec, we need to associate each line with the element, ionization state, and transition responsible, and we need this list in a format that can be interpreted and used by DAOSpec (and then eventually MOOG and MARCS). Since some lines in our observational data of the Sun are unreliable, we cannot simply use all lines identified from the Sun. For example, some lines may be either too weak to read, or are so strong that they oversaturate. Some detected lines are actually noise, cosmic rays, or artifacts introduced by the instrument, misidentified as actual absorption lines. Furthermore, some unwanted lines are also due to molecular absorption from atmosphere. Therefore, we need to check to make sure that all the lines of the previously mentioned atomic data are valid or are otherwise able to be properly identified by our line-fitting software. Additionally, we want to make sure the equivalent

widths measured with DAOSpec of the solar spectrum are consistent with those provided in the solar atlas we use.

Moore's atlas of solar spectral lines (Moore et al. 1966) contains wavelengths of absorption lines, their approximate equivalent widths, their corresponding elements, including the ionization state of those elements, and their excitation potential, (along with other data less relevant to our line list creation). We were able to edit this into a format useable as input for the automatic line-fitting software, DAOSpec.

We next identified and selected certain apertures from the observed spectra, relatively free of noise and artifacts from hardware and with relatively well-defined (unblended) absorption lines, to use for our fitting and line selection. We then ran these apertures (already rectified as described earlier) through DAOSpec, which matched the lines to the Moore data. DAOSpec matches absorption lines it identifies/measures, with lines from the input line list, based on wavelength. To verify the Moore data were reliable, we compared the Moore equivalent widths (EW) with those that DAOSpec measured for corresponding lines. This comparison is show in Figure 4 and includes data points for all apertures used. The relationship is close to a linear 1:1 fit, although as we expect, the data begin to diverge from this relationship more and more at large equivalent widths, and may be due to saturation. Note how much less correlation there is at equivalent widths greater than 120 Å; this is significantly worse at equivalent widths greater than 150 Å. At the shorter wavelengths, the data do indeed confirm a tight 1:1 relation.

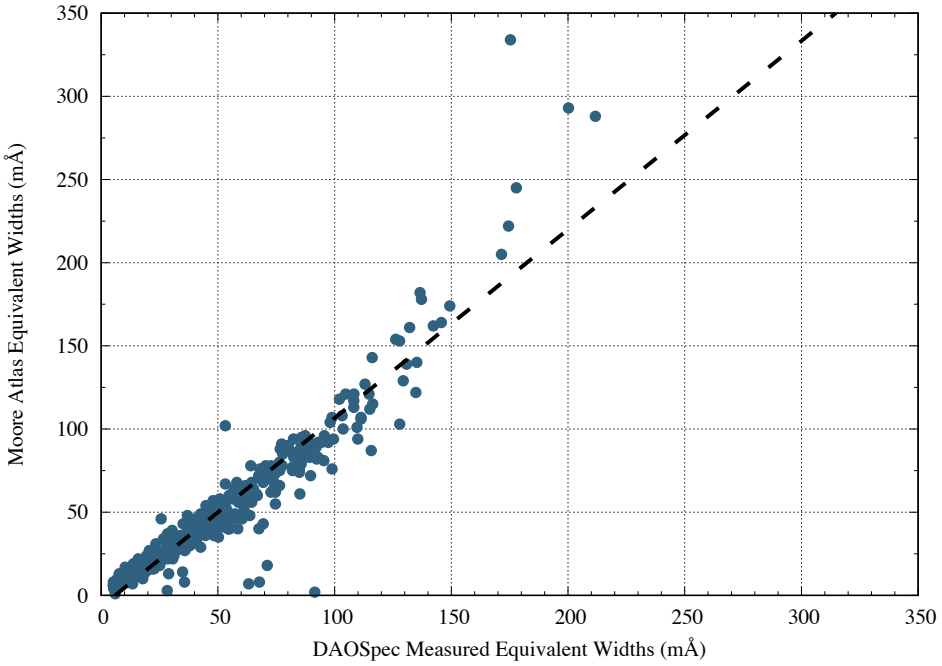

Figure 4: Plot showing linear relation of equivalent widths measured computationally by DAOSpec compared to equivalent widths listed in the Moore atlas. We find a linear best fit line of the form, $y=a+bx$, where y-intercept a=-6.75mÅ and slope b=1.13.

In order to make our collection of measured line info from DAOSpec appropriate for use with both MOOG and MARCS, we also need to include transition probabilities/log *gf* values for the lines in our line list. It is also good to compare the data we obtained from the Moore data with comparable data from another atlas of atomic data to make sure they are consistent. The NIST atlas of atomic line data (Kramida et al. 2018) includes data not limited to only spectral-lines observed from the Sun, but laboratory atomic spectroscopy measurements as well, and is therefore an appropriate choice.

We developed a program that searched through the NIST atomic line data for lines also contained in our solar line list data, and then output all lines from the atlas with wavelengths located within a ±0.06 Å range of the wavelengths measured by DAOSpec of our observational solar data. These selected lines were then compared by hand to the lines in

our line list data to determine which lines from the atlas correctly corresponded to the lines in the line list.

Since the NIST data set contains so much experimental data for many different elements, there may be several lines listed that are all very close together in wavelength (<0.1 Å), but are the result of completely different elements. Because of this, care must be taken to make sure one is not selecting atomic data from the atlas that does not correctly correspond to the lines measured in DAOSpec. This fine selection process is difficult to automate and thus was done by hand for this study. To accomplish this we went through the matched atlas data and determined which lines were correct, based on criteria of: element (the elements in the atlas are represented numerically while the elements from the Moore data are represented in lettered-abbreviations, making it not a simple task to cross-reference them programmatically, though such a task could be done); excitation potential (inconsistency in the formatting of column numbers per row in the Moore data makes it difficult to programmatically parse out the contained excitation potentials); and reasonability of the listed transition probability, given both the line strength (EW) and excitation potential. Occasionally, on lines for which there were no existing identifications in the Moore data, we also considered reasonability of the element to be observed in that portion of the solar spectra — for example, we are not likely to see noble gases in the visible region, or as another example, to see strong lines for molybdenum around 5978 Å instead of strong lines for the significantly more abundant titanium, particularly if no other lines representing members of the molybdenum multiplet have been observed in the rest of the visual spectra.

We followed this procedure for each of the selected apertures. After manually removing results that did not match, we then combined the remaining lines into a single file.

This file was then run through another program we developed that executed a basic "bubble sort" (Knuth 1997) and output the resulting data in the specific formatting necessary for MOOG input. This formatting is also (nearly) acceptable for input to DAOSpec as a line list for use with other stars.

For use as a reference line list for DAOSpec, this file would be run through an additional program (add_trigger_char_for_DAO_input.c), which simply shifts all lines to the left/removes the left-padded blank-space characters of the MOOG formatting, and formats a "#" character at the end of each line so that the lines that DAOSpec identifies with our line list can be easily identified and selected with a "grep" command in our later programs.

3.3.3 Line List Calibration

After assembling this preliminary set of lines, we then needed to prune out any unreliable or misidentified lines in the set. We did this pruning in two ways:

1) We ran the lines through the MOOG software with a model atmosphere generated by MARCS that was appropriate to the Sun, and then investigated and removed lines that resulted in abundance values that deviated greatly from their expected values or which deviated greatly from the values of the other lines. As a hard cutoff, we removed lines that resulted in MOOG output abundances >3σ from the average abundance of other lines of the same element. These deviations were usually the result of either blended lines, misidentified lines (during the step of matching atomic data by hand), or of lines affected by nearby artifacts which made them unreliable for inclusion. Achieving a list of lines from the Sun that produces the appropriate abundance results with MOOG is a critical part of the

line list calibration and ensures that abundances calculated for other stars, whose lines were identified using that line list, can be expected to be reliable.

2) We set a cutoff for inclusion, removing lines that were either too weak to be reliable or distinguishable from noise (EW < 15 mÅ), or that were too strong, making their measurement unreliable by oversaturating the nearby continuum (these required visual inspection, but the typical cutoff was EW > 120 mÅ).

Our final line list based on the Solar spectrum contains 428 lines, of which 251 are Fe I, and 13 are Fe II. In our observed spectra which cover 60 apertures spectrum spanning 3615 Å to 9865 Å, the lines correspond to apertures 10, 12, and 17-30, and include absorption lines in the wavelength ranges of 5310.6 Å to 6767.8 Å, 7386.3 Å to 7498.6 Å, and 7723.2 Å to 7844.6 Å.

To demonstrate and confirm the quality of our line list as well as the quality of a derived model atmosphere, we can look at comparisons of MOOG output abundances for Fe I lines to both the excitation potentials and the reduced widths (RW) of those lines. Ideally, these comparisons would show the derived abundances from different lines to be consistent over varying excitation potentials and reduced equivalent widths. The consistency of abundance over varying excitation potential is related to the reliability of the effective temperature value used in the model (Böcek Topcu et al. 2016). The consistency of abundance over varying reduced equivalent width is related to the reliability of the microturbulence value used in the model (Böcek Topcu et al. 2016). Plots showing these comparisons are shown in Figures 5 and 6. As can be seen, both plots show no apparent trends and a relationship that is very nearly flat.

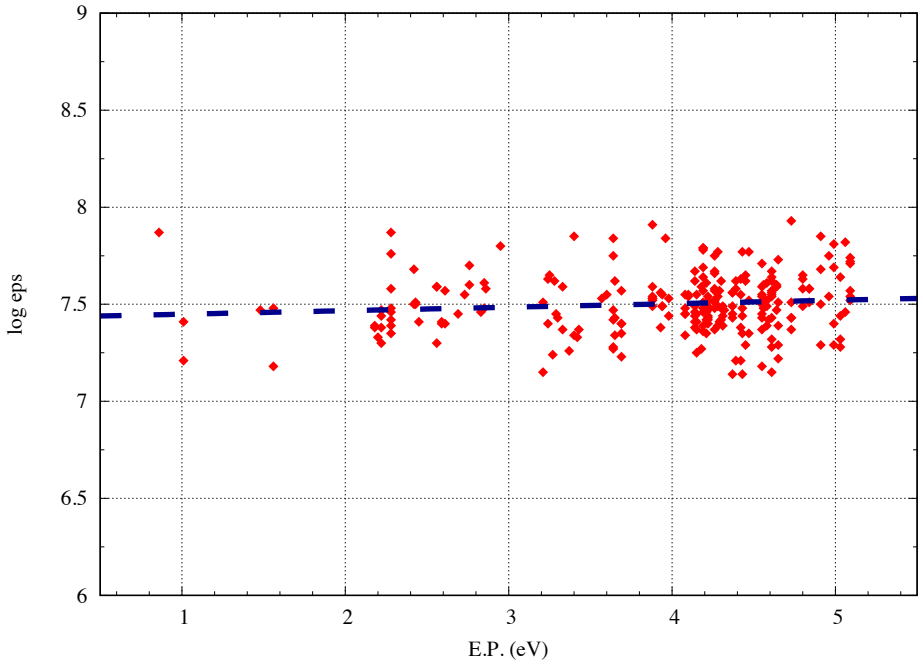

Figure 5: Graph demonstrating accuracy of our Fe-line-derived Solar atmosphere. Flatness of Fe I abundance vs excitation potential relates to quality of the model temperature. Abundances are from MOOG output, using the 12+log(*N*) notation. We fit a straight line having a slope of b = -0.00055 eV^{-1}.

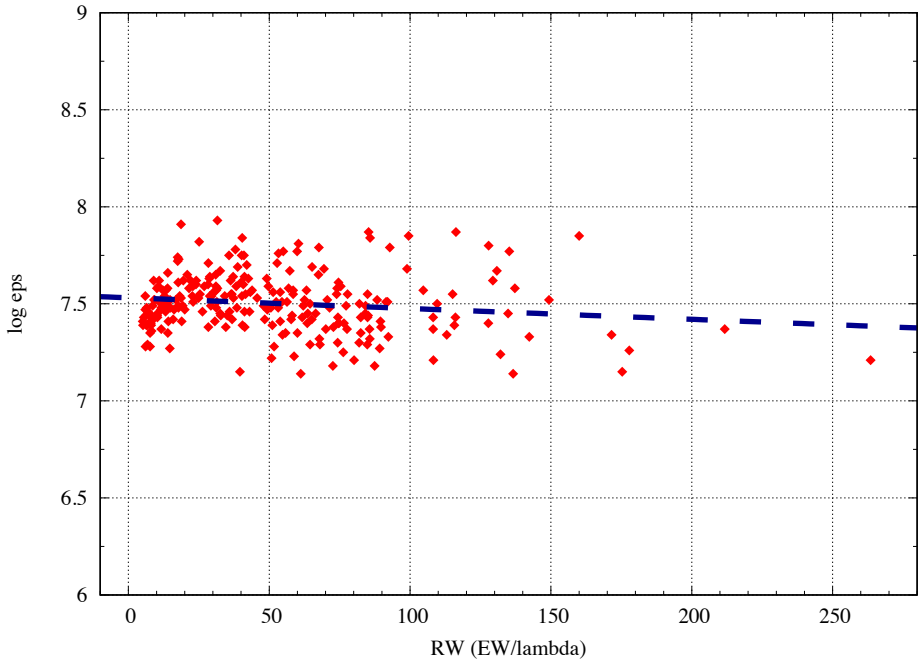

Figure 6: Graph demonstrating accuracy of our Fe-line-derived Solar atmosphere. Flatness of Fe I abundance vs reduced equivalent width relates to quality of the model

microturbulence. Abundances are from MOOG output, using the 12+log(N) notation. We fit a straight line having a slope of b = -0.00056.

3.3.4 Preparation of Program Star Spectra for Abundance Analysis

Following assembly of the reference line list, it is relatively simple to use it to identify absorption lines in the spectra of other program stars through DAOSpec, and then finally use that output with MOOG and MARCS to produce appropriate model atmospheres, stellar parameters, and expected abundances for those stars. We first ran all relevant apertures of our rectified program star spectra (NGC 6940 101 and IC 4756 14) through DAOSpec, using our recently assembled line list. Recall from earlier that "relevant apertures" refers to all apertures within the wavelength ranges covered in our line list. The DAOSpec output for each aperture, containing all measured lines, were then run through another program we developed, which selects only the lines measured by DAOSpec for which there were also matching lines identified from our line list, sorts them, and then outputs them in single file formatted for MOOG input.

The Fe I and Fe II lines from this file were then used as input for the Multimoog wrapper, which iteratively builds a model atmosphere for the star by calling the MARCS and MOOG programs, using the results from each to improve the inputs for the other's next iteration. It employs a "downhill simplex" routine that iterates until it converges on an atmospheric model from MARCS that produces adequately consistent results when used with MOOG on the previously mentioned program star iron lines. The final model also contains our final expected values for atmospheric parameters of effective temperature, surface gravity, and microturbulence for that star.

The final model was then used as the input model for MOOG, which we ran using the complete formatted file of identified lines as input data. The resulting output from MOOG

then outputs expected abundances from each line in the line list from each star. As a final step we removed significantly outlying lines from our input data file, in the same way we did when assembling the line list, removing lines which produced abundances in MOOG >3σ away from the average value of the other lines for that element. Once this procedure was complete, we ran the remaining lines through MOOG again, using the same model atmosphere as before, producing our final abundance analysis for that star. We followed this procedure for each program star.

Chapter 4. Results

After assembling our line list and abundance analysis tools, we tested them on data from two program stars, NGC 6940 101 and IC 4756 14. We present the abundance analysis results here and compare the results from this study to those of others found in literature.

4.1 Atmospheric Parameters

For NGC 6940 101, we found an effective temperature of 5132 K, a surface gravity of 3.13 in terms of log *g*, and a microturbulence of 1.46 km s^{-1}. This agrees well with the values of 5037 K, 3.02, and 1.16 km s^{-1} found in Böcek Topcu et al. (2016). These parameters are summarized in Table 1. Iron abundances for the model in this study were 7.63 and 7.60 (in the 12 + log(*N*) notation) for Fe I and Fe II, respectively.

For IC 4756 14, we found an effective temperature of 4740 K, a surface gravity of 2.48 in terms of log *g*, and a microturbulence of 1.58 km s^{-1}. This too, agrees well with the values of 4720 K, 2.47, and 1.57 km s^{-1} found in Smiljanic et al. (2009). These parameters are summarized in Table 2. Iron abundances for the model were 7.47 (again, in the 12 + log(*N*) notation) for both Fe I and Fe II. Our values for atmospheric parameters, especially for IC 4756 14, are in close agreement with those found in previous studies.

Table 1
Comparison of Atmospheric Parameters for NGC 6940 101

Reference	$T_{\rm eff}$ (K)	log *g*	Microturbulence (km s^{-1})
This Study	5132	3.13	1.46
Böcek Topcu et al. (2016)	5037	3.02	1.16

Table 2
Comparison of Atmospheric Parameters for IC 4765 14

Reference	T_{eff} (K)	log g	Microturbulence (km s^{-1})
This Study	4740	2.48	1.58
Smiljanic et al. (2009)	4720	2.47	1.57

4.2 Abundances

4.2.1 NGC 6940 101

A full list of abundances found for NGC 6940 101 with comparisons to previous values found in literature is given in Table 3. Uncertainty values for abundances and number of lines measured are not given in the Böcek Topcu et al. paper (2016), and so the uncertainty given in this table is entirely from our own data.

Our values for manganese stick out as being relatively further from the other literature values than other elements. Although it is not horrible, it is significantly less reliable than all of our other elements. The reasons for this are likely due to poor log *gf* values measured for manganese. Böcek Topcu et al. (2016) points out that there is an Fe I line at 6016.61 Å that is blended with the manganese hyperfine structure around 6016 Å, which creates "an unrealistic asymmetric line profile around the Mn I components" that can affect abundance determinations from that line, leading to scattered and internally inconsistent results with other manganese lines. They resolved this problem by using the spectral synthesis method on this region. Aside from manganese, the other outliers in our data when compared to the literature are from copper, aluminum, and cobalt. Of those, there are not enough lines of copper measured from our data to determine a statistical uncertainty, and the statistical error-bars for cobalt show that our abundance value and the literature value are within the uncertainty. Not including manganese, the differences in abundances for

aluminum, silicon, and scandium do fall outside of the range covered by statistical uncertainty, though the differences are small, and both silicon as well as scandium are indeed among the elements whose differences in abundance from previously found values are nearest to zero. A plot with the differences in abundances for NGC 6940 101 between this paper and the Böcek Topcu et al. (2016) paper can be found in Figure 7.

We are able to produce detailed abundance information on most n-capture products and some of the lighter s-process products. To produce abundance details for heavier s-process and r-process elements, we would need spectrographic data at shorter wavelengths. Furthermore, it would be necessary to expand the line list to be able to identify lines at those wavelengths.

Table 3
NGC 6940 101 abundances

Element	[X/Fe][1]	# of Lines[1]	[X/Fe][2]	# of Lines[2]	Difference	Weighted Uncertainty
11 Na	0.11	3	0.06	...	0.05	0.14
12 Mg	-0.07	5	-0.02	...	-0.05	0.19
13 Al	-0.18	3	-0.03	...	-0.15	0.12
14 Si	0.026	14	0.12	...	-0.094	0.079
20 Ca	-0.07	6	0.04	...	-0.11	0.21
21 Sc	-0.04	3	0.04	...	-0.08	0.07
22 Ti	-0.078	15	-0.06	...	-0.018	0.13
23 V	0.04	9	-0.04	...	0.08	0.17
24 Cr	-0.04	16	0.028	...	-0.068	0.173
25 Mn	0.29	6	-0.13	...	0.42	0.22
26 Fe	-0.011	219	0.089	...	-0.10	0.149
27 Co	-0.23	5	-0.09	...	-0.14	0.2
28 Ni	-0.01	36	-0.01	...	0	0.15
29 Cu	0.07	1	-0.10	...	0.17	0

Notes: Column 1, labeled "Element," makes it easier to be programmatically parsed, by first giving atomic number, followed by abbreviation. Columns 2 and 4 give abundances from respective studies, using the [X/Fe] notation. Columns 3 and 5 give the number of absorption lines used to determine abundances for the respective studies. Column 6 gives the difference in abundance values found between the two studies. Column 7 gives the uncertainty for column 6, combining the uncertainties from both studies in a weighted

uncertainty where possible. For abundances for which there was data from multiple ionization states of the same element, the abundance value is given as a weighted average of the states.
References: (1) This study; (2) Böcek Topcu et al. (2016).

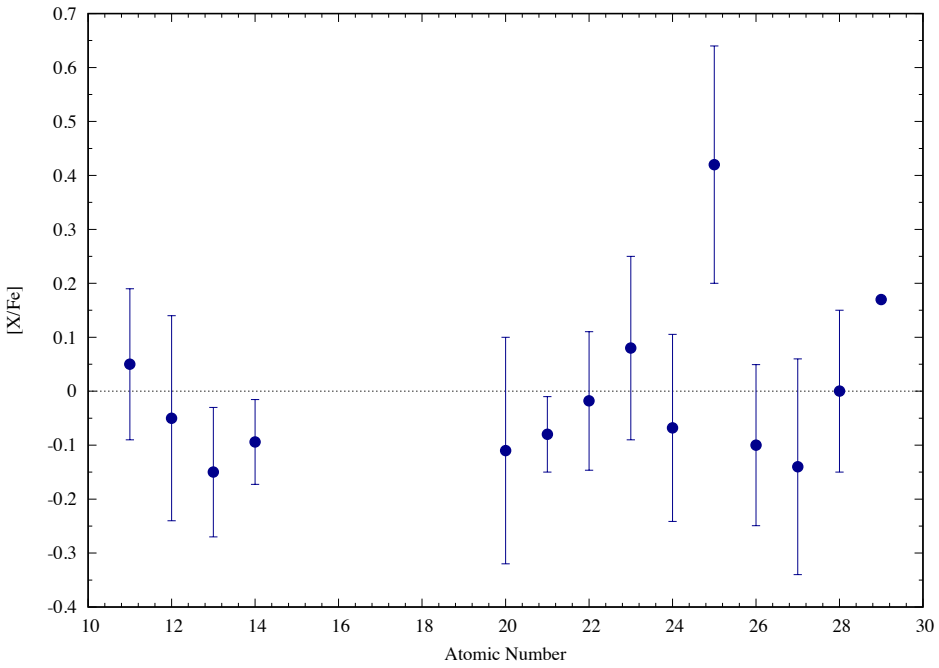

Figure 7: Plot for NGC 6940 101 showing the difference between our abundance results and those derived in Böcek Topcu et al. (2016). Error bars show the uncertainty on derived abundances. Points with no uncertainty given are based on 2 or fewer lines.

4.2.2 IC 4756 14

A full list of abundances found for IC 4756 14 with comparisons to previous values found in literature is given in Table 4. In contrast to the data for NGC 6940 101 in the Böcek Topcu et al. (2016) paper, the Smiljanic et al. (2009) data for IC 4756 14 does not include data for manganese, but does include the number of lines used for each element as well as the statistical uncertainty for their abundance values.

Again, the values we found for this star agree well with previously determined values in literature. The largest outliers here are scandium, chromium, and cobalt. These elements have both the largest differences between our values and those found in the literature, as well as values that fall the farthest out of uncertainty from each other. We notice that — with the

exception of cobalt — our abundance values are all based off of more measured absorption lines than those in Smiljanic et al. (2009). A plot with the differences in abundances for IC 4756 14 between this paper and the Smiljanic et al. (2009) paper can be found in Figure 8.

Table 4
IC 4756 14 abundances

Element	[X/Fe][2]	# of Lines[1]	[X/Fe][2]	# of Lines[2]	Difference	Weighted Uncertainty
11 Na	-0.01	3	…	…	…	0.16
12 Mg	-0.27	3	-0.05	1	-0.22	0.12
13 Al	-0.28	3	…	…	…	0.12
14 Si	-0.05	10	0.10	7	-0.15	0.10
20 Ca	-0.22	5	0.03	5	-0.25	0.14
21 Sc	-0.25	3	0.19	2	-0.44	0.06
22 Ti	-0.19	10	-0.03	9	-0.16	0.12
23 V	-0.08	10	0.09	8	-0.17	0.16
24 Cr	-0.25	14	0.11	3	-0.36	0.15
25 Mn	0.29	7	…	…	…	0.26
26 Fe	-0.15	201	0.03	41	-0.18	0.16
27 Co	-0.21	5	0.12	8	-0.33	0.17
28 Ni	-0.16	35	0.03	9	-0.19	0.12
29 Cu	0.46	2	…	…	…	…

Notes: IC 4756 14 abundances
Follows the same column conventions as Table 3. See notes for Table 3 for a more complete description. For abundances for which there was data from multiple ionization states of the same element, the abundance value is given as a weighted average of the states.
References: (1) This study; (2) Smiljanic et al. (2009).

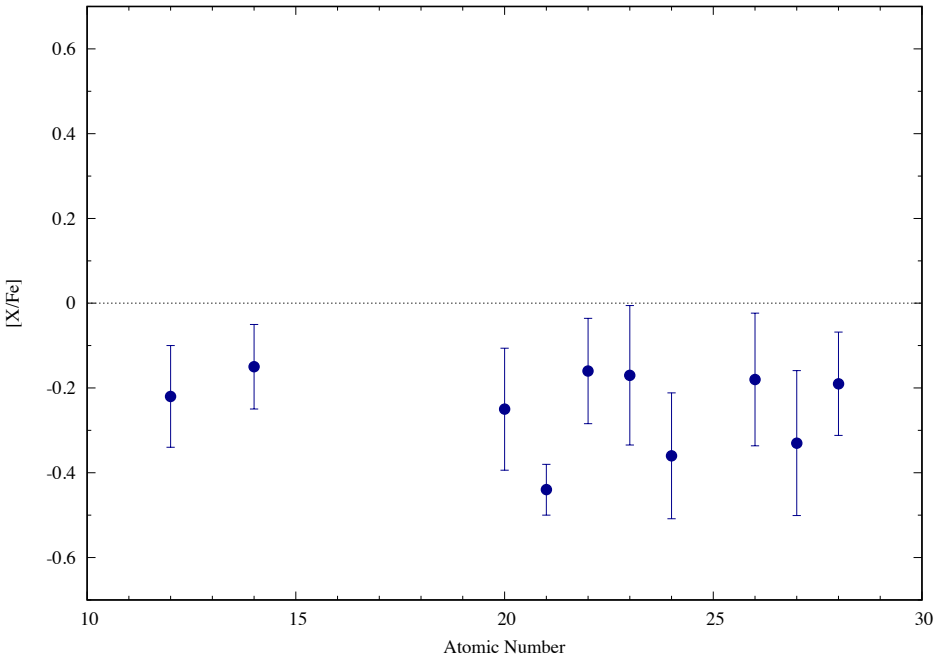

Figure 8: Plot for IC 4756 14 showing the difference between our abundance results and those derived in Smiljanic et al. 2009. Error bars show the uncertainty on derived abundances.

4.3 Discussion

While abundance results for both stars compare well to those found in literature, there is a noticeable trend in our results to be slightly underabundant when compared to the other studies. The trend for our data to be underabundant with respect to previously reported values is more apparent for IC 4756 14 than for NGC 6940 101, but it does seem to exist in both. This is something that should be investigated in future work, by increasing our sample size and determining abundances for an increased number of stars and observing if this trend is present in comparisons of results for those stars as well. One potential source of the trend, worth looking into further, may be the accuracy of atomic data used for the line list of each study. For example, Smiljanic et al. (2009) offers as a source of error that their log *g* values may have been slightly overestimated, resulting in overestimated abundances as well. Our study does use a somewhat older set of data (Moore et al. 1966) for line identification, which

may be less accurate, but as described in Chapter 3, these data were then backed up with and checked against more recent observational and experimental atomic data from NIST (Kramida et al. 2018).

In general, potential future work could include analysis of more stars from the same clusters used in this paper (NGC 6940 and IC 4756) to produce more detailed survey information about those clusters. This additional data could also be used to better define the quality of results produced using our analysis tools, especially with respect to other studies. Additionally, there are also numerous places in our analysis process where additional code could be implemented to further streamline and automate the analysis process. Another useful area of improvement could be expanding the range of use of our line list, by adding additional lines from other apertures. This itself would be useful in the development of future work and could expand the types of stars that can be analyzed successfully with our tools. Finally, it is worth considering combining our automatic equivalent width measuring method with the synthetic spectra method (described briefly in Chapter 2) to obtain abundances for lines beyond our available wavelength range and for elements for which there are few observable lines, such as lithium (Gray 2005), but that are still of significant interest to researchers.

Chapter 5. Conclusion

Abundance analysis of elements in stars and clusters has relevance to many topics in stellar, galactic, and nuclear astrophysics, and allows us to draw conclusions about the histories of those objects. Traditional methods of performing such studies have the potential to be quite time-consuming, and this limitation will only be exacerbated by the massive amounts of data that will be produced as astronomical surveys continue to grow in size and capability. Finding ways to automate this analysis provides researchers with tools to efficiently handle and process large data sets of high-resolution spectra.

In an attempt to address these concerns, we developed a reference "line list" — composed of 428 atomic transitions and calibrated with data from the Sun — for use with the spectral-line fitting software DAOSpec, in order to allow the software to properly identify measured absorption lines. We also developed some programs to semi-automate a method to determine abundances and stellar atmospheric parameters of effective temperature, surface gravity, and microturbulence, from the combined use of the line list with DAOSpec, the MARCS grid of model atmospheres, and the MOOG spectral-line analysis software.

We used this line list and semi-automated method to conduct abundance analyses on two stars — NGC 6940 101 and IC 4756 14 — and compared the results to those previously described in the literature, in order to better illustrate and confirm the reliability of our tools. For NGC 6940 101, we determined atmospheric parameters of $T_{\rm eff}$ = 5132 K, log g = 3.13, and microturbulence = 1.46 km s^{-1}, which is in good agreement with those found in Böcek Topcu et al. (2016). For IC 4756 14, we determined atmospheric parameters of $T_{\rm eff}$ = 4760 K, log g = 2.48, and microturbulence = 1.58 km s^{-1}. These too agree closely with previously

published results, found in Smiljanic et al. (2009). Despite an apparent trend for our derived abundances for both stars to be slightly underabundant relative to the previously predicted values found in the literature, more so for IC 4756 14, we find that our derived abundances still agree relatively well with their values.

Future work using our presented line list and tools from in this paper should continue analyzing and comparing abundance results from more stars in order to build a larger sample size from which to compare the performance of our tools, while also paying close attention to see if a consistent trend towards relative underabundance is present. If such a trend is found, effort should be made to resolve it. Ideal further improvement for the methods described in this paper would focus on adding more transitions to the line list to expand its range of use over more wavelengths, while attempts to complement our method with the synthetic spectra method could also significantly expand our range of available elements.

Chapter 6. Bibliography

6.1 Works Cited

Böcek Topcu, G., Afşar, M., & Sneden, C. 2016, Monthly Notices of the Royal Astronomical Society, 463, 580

Böhm-Vitense, E. 1989, Introduction to Stellar Astrophysics: Volume 1, Basic Stellar Observations and Data (Cambridge University Press)

Gray, D. F. 2005, The Observation and Analysis of Stellar Photospheres (Cambridge University Press)

Gray, R. O., & Corbally, C. J. 1994, The Astrophysical Journal, 107, 742

Gustafsson, B., Bell, R. A., Eriksson, K., & Nordlund, A. 1975, Astronomy and Astrophysics, 42, 407

Knuth, D. E. 1997, The Art of Computer Programming: Sorting and searching (Pearson Education)

Kramida, A., Ralchenko, Y., Reader, J., & and NIST ASD Team. 2018, NIST Atomic Spectra Database (ver. 5.5.6), [Online] (Gaithersburg, MD: National Institute of Standards and Technology), https://physics.nist.gov/asd

Kurucz, R. L., & Avrett, E. H. 1981, SAO Special Report, 391

Moore, C. E., Minnaert, M. G. J., & Houtgast, J. 1966, The solar spectrum 2935 A to 8770 A

Smiljanic, R., Gauderon, R., North, P., et al. 2009, Astronomy and Astrophysics, 502, 267

Sneden, C. 1973, The Astrophysical Journal, 184, 839

Stetson, P. B., & Pancino, E. 2008, Publications of the Astronomical Society of the Pacific, 120, 1332

Tull, R. G., MacQueen, P. J., Sneden, C., & Lambert, D. L. 1995, Publications of the Astronomical Society of the Pacific, 107, 251

6.2 Works Consulted

Afşar, M., Sneden, C., Frebel, A., et al. 2016, The Astrophysical Journal, 819, 103

Allende Prieto, C., & Lopez, R. J. G. 1998, Astronomy and Astrophysics Supplement Series, 131, 431

Boesgaard, A. M., Lum, M. G., Deliyannis, C. P., et al. 2016, The Astrophysical Journal, 830, 49

Carretta, E., Bragaglia, A., Lucatello, S., et al. 2017, VizieR Online Data Catalog, 360, http://adsabs.harvard.edu/abs/2017yCat..36000118C

Cummings, J. D., Deliyannis, C. P., Maderak, R. M., & Steinhauer, A. 2017, The Astronomical Journal, 153, 128

Hansen, C. J., Jofré, P., Koch, A., McWilliam, A., & Sneden, C. S. 2017, Astronomy and Astrophysics, 598, A54

Heiter, U., Soubiran, C., Netopil, M., & Paunzen, E. 2014, Astronomy and Astrophysics, 561, A93

Lee-Brown, D. B., Anthony-Twarog, B. J., Deliyannis, C. P., Rich, E., & Twarog, B. A. 2015, The Astronomical Journal, 149, 121

Mikolaitis, Š., Tautvaišienė, G., Gratton, R., Bragaglia, A., & Carretta, E. 2011, Monthly Notices of the Royal Astronomical Society, 413, 2199

Pancino, E., & Stetson, P. B. 2008, Cooking with DAOSPEC, http://www.arcetri.inaf.it/%7Epancino/Docs/daospec.pdf

Reddy, A. B. S., Lambert, D. L., & Giridhar, S. 2016, Monthly Notices of the Royal Astronomical Society, 463, 4366

Roederer, I. U., Preston, G. W., Thompson, I. B., Shectman, S. A., & Sneden, C. 2014, The Astrophysical Journal, 784, 158

Siqueira-Mello, C., Spite, M., Barbuy, B., et al. 2016, Journal of Physics: Conference Series, 665, 012056

Sneden, C., Bean, J., Ivans, I., Lucatello, S., & Sobeck, J. 2012, Astrophysics Source Code Library, http://adsabs.harvard.edu/abs/2012ascl.soft02009S

Sneden, C., Lawler, J. E., Hartog, E. A. D., & Wood, M. E. 2015, Proceedings of the International Astronomical Union

Waters, C. Z., & Hollek, J. K. 2013, Publications of the Astronomical Society of the Pacific, 125, 1164

Wood, M. P., Sneden, C., Lawler, J. E., et al. 2018, The Astrophysical Journal Supplement Series, 234, http://adsabs.harvard.edu/abs/2018ApJS..234...25W

Appendix A

line_data_sort.c

```
/*    David Gribble, 9/18/2017

Step1
Reads in data from a daospec output file and a dump of line data that
has already been grabbed from a database, and compares the wavelengths
of each line from the line data file to the identified lines in the
daospec output, printing out to a file only the lines from the line
data file that are within a certain range of the daospec identified
lines. The daospec wavelength is also included on the printed out
lines.  Each line is (aside from the extra wavelength value from the
line data dump) formatted for Moog input.
*/

#include <stdio.h>
#include <stdlib.h>
#include <math.h>
#include <time.h>

int main()
{
      double lambda[100], lambda_correct[100], delta_lambda[100];
      double lambda_lindat[35800], log_gf[35800], elem_ion[35800],
excit_pot_lower[35800];

      int N = 0;
      int M = 0;
      int i, j;

      FILE *in1, *in2;
      FILE *out1;

      char dum;
      char buf[1000];

      /* open input & output textfiles for both data sets for writing
later */
      if((in1 = fopen("norm_Solar+filt.daospec", "r")) == NULL){
            printf("\nCannot open file for input\n");
      }
      if((in2 = fopen("line_data_short.out", "r")) == NULL){
            printf("\nCannot open file for input\n");
      }
      if ((out1 = fopen("line_list.txt", "w")) == NULL){
            printf("\nCannot open file for output\n");
      }

      while ((dum = getc(in1)) != '\n'){
            printf("dum=%c\n", dum);
```

```
      };
printf("line 1 skipped\n");
      while ((dum = getc(in1)) != '\n'){
      };          //read & skip first 2 lines
printf("line 2 skipped\n");

      while(fscanf(in1,"%lf %lf %lf", &lambda[M], &lambda_correct[M],
&delta_lambda[M]) != EOF){
            printf("%7.3lf   %7.3lf      %4.1lf      M=%d\n", lambda[M],
lambda_correct[M], delta_lambda[M], M);
            M=M+1;
            fgets(buf, 1000, in1);
      }
      fclose(in1);
      printf("file 1 scan complete M=%d\n", M);

      while(fscanf(in2,"%lf %lf %lf %lf", &lambda_lindat[N],
&log_gf[N], &elem_ion[N], &excit_pot_lower[N]) != EOF){
            printf("%7.4lf   %4.3lf      %4.2lf      %lf   N=%d\n",
lambda_lindat[N], log_gf[N], elem_ion[N], excit_pot_lower[N], N);
            N=N+1;
      }
      fclose(in2);
      printf("file 2 scan complete N=%d\n", N);

      for(i=0;i<N;i=i+1){
            lambda_lindat[i] = lambda_lindat[i] * 10;     //convert from
nm to angstroms
      }

      fprintf(out1, "Solar+filt,   David Gribble,   1/02/18\n");

      for(i=0;i<N;i=i+1){
            for(j=0;j<M;j=j+1){
                  if ((lambda_lindat[i] >= lambda_correct[j]-0.06) &&
(lambda_lindat[i]<= lambda_correct[j]+0.06)){
                        fprintf(out1, "   %6.2lf %7.3lf      %04.1lf
%05.2lf     % 06.2lf                        %05.1lf\n",
lambda_correct[j], lambda_lindat[i], elem_ion[i], excit_pot_lower[i],
log_gf[i], delta_lambda[j]);
/*
%[space] forces to print out '-' for negatives and a space for
positives; %0 prints leading zeros if number has less than specified
width; %# specifies total width, including before & after decimal and
the decimal itself (and I believe also includes +/- signs when they
appear); %.# specifies number of characters after the decimal
*/
                  }
            }
      }
      fclose(out1);

return(0);
}
```

Appendix B

```
                        line_list_concact_sort.c
/*    David Gribble, 9/18/2017

Step2
Reads in data from the concatenated file of line data and daospec
output for all selected apertures, and sorts into final Moog line list
file, in ascending order of element and ionization state, and then
wavelength. Also discards line data wavelength from input file and
keeps the corresponding daospec radial velocity corrected wavelength.
Each line is (aside from the extra wavelength value from the line data
dump) formatted for Moog input.

*/

#include <stdio.h>
#include <stdlib.h>
#include <math.h>
#include <time.h>

int main()
{
      double lambda_correct[1000], delta_lambda[1000];
      double lambda_lindat[1000], log_gf[1000], elem_ion[1000],
excit_pot_lower[1000];

      int N = 0;
      int i, j;

      FILE *in1;
      FILE *out1;

      double dummy;
      char dum;

      /* open input & output textfiles for the data set for writing
later */
      if((in1 = fopen("line_list_concact.txt", "r")) == NULL){
            printf("\nCannot open file for input\n");
      }
      if ((out1 = fopen("line_list_full_sorted.txt", "w")) == NULL){
            printf("\nCannot open file for output\n");
      }

      //read & skip over first line/header
      while ((dum = getc(in1)) != '\n'){
            printf("dum=%c\n", dum);
      };
      printf("line 1 skipped\n");  //for debug
```

```
      while(fscanf(in1,"%lf %lf %lf %lf %lf %lf", &lambda_correct[N],
&lambda_lindat[N], &elem_ion[N], &excit_pot_lower[N], &log_gf[N],
&delta_lambda[N]) != EOF){
            printf("%7.2lf   %7.3lf     %03.1lf %05.2lf %06.2lf %05.1lf
      M=%d\n", lambda_correct[N], lambda_lindat[N], elem_ion[N],
excit_pot_lower[N], log_gf[N], delta_lambda[N], N); //for debug
//          fgets(buf, 1000, in1); //for skipping to end of line for
poorly formatted/troublesome input files
            N=N+1;
      }
      fclose(in1);
      printf("file 1 scan complete N=%d\n", N);     //for debug

      fprintf(out1, "Solar+filt,   David Gribble,   01/22/18\n");

      for(i=0;i<N;i=i+1){
            for(j=i+1;j<N;j=j+1){
                  if (elem_ion[i] > elem_ion[j]){
                        dummy = elem_ion[i];
                        elem_ion[i] = elem_ion[j];
                        elem_ion[j] = dummy;

                        dummy = lambda_correct[i];
                        lambda_correct[i] = lambda_correct[j];
                        lambda_correct[j] = dummy;

                        dummy = lambda_lindat[i];
                        lambda_lindat[i] = lambda_lindat[j];
                        lambda_lindat[j] = dummy;

                        dummy = excit_pot_lower[i];
                        excit_pot_lower[i] = excit_pot_lower[j];
                        excit_pot_lower[j] = dummy;

                        dummy = log_gf[i];
                        log_gf[i] = log_gf[j];
                        log_gf[j] = dummy;

                        dummy = delta_lambda[i];
                        delta_lambda[i] = delta_lambda[j];
                        delta_lambda[j] = dummy;
                  }
                  else if ((elem_ion[i] == elem_ion[j]) &&
(lambda_correct[i] > lambda_correct[j])){
//                      if (lambda_correct[i] > lambda_correct[j]){
                              dummy = elem_ion[i];
                              elem_ion[i] = elem_ion[j];
                              elem_ion[j] = dummy;
                              //printf("elem_ion[%d]=%lf\n", i,
elem_ion[i]);    //for debug

                              dummy = lambda_correct[i];
                              lambda_correct[i] = lambda_correct[j];
                              lambda_correct[j] = dummy;
```

```
                              dummy = lambda_lindat[i];
                              lambda_lindat[i] = lambda_lindat[j];
                              lambda_lindat[j] = dummy;

                              dummy = excit_pot_lower[i];
                              excit_pot_lower[i] = excit_pot_lower[j];
                              excit_pot_lower[j] = dummy;

                              dummy = log_gf[i];
                              log_gf[i] = log_gf[j];
                              log_gf[j] = dummy;

                              dummy = delta_lambda[i];
                              delta_lambda[i] = delta_lambda[j];
                              delta_lambda[j] = dummy;
//                        }
                  }
            }
      }


            //could probably just include this within previous for loop
at end of the logic in order to save time/mem, but let's leave outside
for now to be safe
            for(i=0;i<N;i=i+1){
                  fprintf(out1, "   %6.2lf      %04.1lf    %05.2lf     %
06.2lf                          %05.1lf\n", lambda_correct[i],
elem_ion[i], excit_pot_lower[i], log_gf[i], delta_lambda[i]);
            }
/*
%[space] forces to print out '-' for negatives and a space for
positives; %0 prints leading zeros if number has less than specified
width; %# specifies total width, including before & after decimal and
the decimal itself (and I believe also includes +/- signs when they
appear); %.# specifies number of characters after the decimal
*/

      fclose(out1);

      printf("\nTask complete\n");

return(0);
}
```

Appendix C

```
                    add_trigger_char_for_DAO_Input.c
/*    David Gribble, 9/18/2017

Step3
Shifts line_list_full_sorted.txt left for formatting with DAOSpec; adds
a "#" char to the end of each line, to trigger on in order to remove
lines from daospec output afterward by using the grep command

*/

#include <stdio.h>
#include <stdlib.h>
#include <math.h>
#include <time.h>

int main()
{
      double lambda_correct[1000], delta_lambda[1000];
      double lambda_lindat[1000], log_gf[1000], elem_ion[1000],
excit_pot_lower[1000];

      int N = 0;
      int i, j;

      FILE *in1;
      FILE *out1;

      double dummy;
      char dum;
//    char buf[1000];

      /* open input & output textfiles for the data set for writing
later */
      if((in1 = fopen("line_list_full_sorted.txt", "r")) == NULL){
            printf("\nCannot open file for input\n");
      }
      if ((out1 = fopen("laboratory.dat", "w")) == NULL){
            printf("\nCannot open file for output\n");
      }

      //read & skip over first line/header
      while ((dum = getc(in1)) != '\n'){
            printf("dum=%c\n", dum);
      };
      printf("line 1 skipped\n");  //for debug

      while(fscanf(in1,"%lf %lf %lf %lf %lf", &lambda_correct[N],
&elem_ion[N], &excit_pot_lower[N], &log_gf[N], &delta_lambda[N]) !=
EOF){
```

```
            printf("%7.2lf   %03.1lf %05.2lf %06.2lf %05.1lf   M=%d\n",
lambda_correct[N], elem_ion[N], excit_pot_lower[N], log_gf[N],
delta_lambda[N], N);   //for debug
//          fgets(buf, 1000, in1); //for skipping to end of line for
poorly formatted/troublesome input files
            N=N+1;
      }
      fclose(in1);
      printf("file 1 scan complete N=%d\n", N);     //for debug

      fprintf(out1, "Solar+filt,   David Gribble,   03/6/18\n");

      for(i=0;i<N;i=i+1){
            for(j=i+1;j<N;j=j+1){
                  if (elem_ion[i] > elem_ion[j]){
                        dummy = elem_ion[i];
                        elem_ion[i] = elem_ion[j];
                        elem_ion[j] = dummy;

                        dummy = lambda_correct[i];
                        lambda_correct[i] = lambda_correct[j];
                        lambda_correct[j] = dummy;

                        dummy = excit_pot_lower[i];
                        excit_pot_lower[i] = excit_pot_lower[j];
                        excit_pot_lower[j] = dummy;

                        dummy = log_gf[i];
                        log_gf[i] = log_gf[j];
                        log_gf[j] = dummy;

                        dummy = delta_lambda[i];
                        delta_lambda[i] = delta_lambda[j];
                        delta_lambda[j] = dummy;
                  }
                  else if ((elem_ion[i] == elem_ion[j]) &&
(lambda_correct[i] > lambda_correct[j])){
//                      if (lambda_correct[i] > lambda_correct[j]){
                              dummy = elem_ion[i];
                              elem_ion[i] = elem_ion[j];
                              elem_ion[j] = dummy;
                              //printf("elem_ion[%d]=%lf\n", i,
elem_ion[i]);    //for debug

                              dummy = lambda_correct[i];
                              lambda_correct[i] = lambda_correct[j];
                              lambda_correct[j] = dummy;

                              dummy = excit_pot_lower[i];
                              excit_pot_lower[i] = excit_pot_lower[j];
                              excit_pot_lower[j] = dummy;

                              dummy = log_gf[i];
                              log_gf[i] = log_gf[j];
```

```
                              log_gf[j] = dummy;

                              dummy = delta_lambda[i];
                              delta_lambda[i] = delta_lambda[j];
                              delta_lambda[j] = dummy;
//                        }
                    }
               }
          }


          //could probably just include this within previous for loop
at end of the logic in order to save time/mem, but let's leave outside
for now to be safe
          for(i=0;i<N;i=i+1){
               fprintf(out1, "%6.2lf      %04.1lf    %05.2lf     %
06.2lf                         %05.1lf  #\n", lambda_correct[i],
elem_ion[i], excit_pot_lower[i], log_gf[i], delta_lambda[i]);
          }
/*
%[space] forces to print out '-' for negatives and a space for
positives; %0 prints leading zeros if number has less than specified
width; %# specifies total width, including before & after decimal and
the decimal itself (and I believe also includes +/- signs when they
appear); %.# specifies number of characters after the decimal
*/

     fclose(out1);

     printf("\nTask complete\n");

return(0);
}
```

Appendix D

```
                    line_list_concact_sort_NGC6940.c
/*    David Gribble, 1/23/2018
Step2
Reads in data from the concatenated file of line data and daospec
output for all selected apertures, and sorts into final Moog line list
file, in ascending order of element and ionization state, and then
wavelength. Also discards line data wavelength from input file and
keeps the corresponding daospec radial velocity corrected wavelength.
Each line is (aside from the extra wavelength value from the line data
dump) formatted for Moog input.
*/

#include <stdio.h>
#include <stdlib.h>
#include <math.h>
#include <time.h>

int main()
{
      double lambda_correct[1000], delta_lambda[1000];
      double lambda_lindat[1000], log_gf[1000], elem_ion[1000],
excit_pot_lower[1000];
      double abra, kadabra, alakazam, crucio;

      int N = 0;
      int i, j;

      FILE *in1;
      FILE *out1;

      double dummy;
      char dum;
      char buf[1000];

//can comment these three lines out if no new lines from daospec output
to add to the unsorted list
      system("cp norm_NGC6940101.daospec foo.out");
      system("grep '#' foo.out > norm_NGC6940101.daospec");
      system("grep '#' foo.out >> norm_NGC6940101.daospec.main");

      /* open input & output textfiles for the data set for writing
later */
      if((in1 = fopen("norm_NGC6940101.daospec.main", "r")) == NULL){
            printf("\nCannot open file for input\n");
      }
      if ((out1 = fopen("line_list_NGC6940_full_sorted.txt", "w")) ==
NULL){
            printf("\nCannot open file for output\n");
      }
```

```
      while(fscanf(in1,"%lf %lf %lf %lf %lf %lf %lf %lf %lf", &abra,
&lambda_correct[N], &delta_lambda[N], &kadabra, &alakazam, &crucio,
&elem_ion[N], &excit_pot_lower[N], &log_gf[N]) != EOF){
            printf("%7.2lf   %7.3lf     %03.1lf %05.2lf %06.2lf %05.1lf
      M=%d\n", lambda_correct[N], lambda_lindat[N], elem_ion[N],
excit_pot_lower[N], log_gf[N], delta_lambda[N], N); //for debug
//          fgets(buf, 1000, in1); //for skipping to end of line for
poorly formatted/troublesome input files
            N=N+1;
            fgets(buf, 1000, in1);
      }
      fclose(in1);
      printf("file 1 scan complete N=%d\n", N);     //for debug

      fprintf(out1, "NGC6940 101,  David Gribble,   02/6/18\n");

      for(i=0;i<N;i=i+1){
            for(j=i+1;j<N;j=j+1){
                  if (elem_ion[i] > elem_ion[j]){
                        dummy = elem_ion[i];
                        elem_ion[i] = elem_ion[j];
                        elem_ion[j] = dummy;

                        dummy = lambda_correct[i];
                        lambda_correct[i] = lambda_correct[j];
                        lambda_correct[j] = dummy;

                        dummy = lambda_lindat[i];
                        lambda_lindat[i] = lambda_lindat[j];
                        lambda_lindat[j] = dummy;

                        dummy = excit_pot_lower[i];
                        excit_pot_lower[i] = excit_pot_lower[j];
                        excit_pot_lower[j] = dummy;

                        dummy = log_gf[i];
                        log_gf[i] = log_gf[j];
                        log_gf[j] = dummy;

                        dummy = delta_lambda[i];
                        delta_lambda[i] = delta_lambda[j];
                        delta_lambda[j] = dummy;
                  }
                  else if ((elem_ion[i] == elem_ion[j]) &&
(lambda_correct[i] > lambda_correct[j])){
//                      if (lambda_correct[i] > lambda_correct[j]){
                              dummy = elem_ion[i];
                              elem_ion[i] = elem_ion[j];
                              elem_ion[j] = dummy;
                              //printf("elem_ion[%d]=%lf\n", i,
elem_ion[i]);    //for debug

                              dummy = lambda_correct[i];
                              lambda_correct[i] = lambda_correct[j];
```

```
                              lambda_correct[j] = dummy;

                              dummy = lambda_lindat[i];
                              lambda_lindat[i] = lambda_lindat[j];
                              lambda_lindat[j] = dummy;

                              dummy = excit_pot_lower[i];
                              excit_pot_lower[i] = excit_pot_lower[j];
                              excit_pot_lower[j] = dummy;

                              dummy = log_gf[i];
                              log_gf[i] = log_gf[j];
                              log_gf[j] = dummy;

                              dummy = delta_lambda[i];
                              delta_lambda[i] = delta_lambda[j];
                              delta_lambda[j] = dummy;
//                        }
                  }
            }
      }


            //could probably just include this within previous for loop
at end of the logic in order to save time/mem, but let's leave outside
for now to be safe
            for(i=0;i<N;i=i+1){
                  fprintf(out1, "   %6.2lf      %04.1lf    %05.2lf     %
06.2lf                        %05.1lf\n", lambda_correct[i],
elem_ion[i], excit_pot_lower[i], log_gf[i], delta_lambda[i]);
            }
/*
%[space] forces to print out '-' for negatives and a space for
positives; %0 prints leading zeros if number has less than specified
width; %# specifies total width, including before & after decimal and
the decimal itself (and I believe also includes +/- signs when they
appear); %.# specifies number of characters after the decimal
*/

      fclose(out1);

      printf("\nTask complete\n");

return(0);
}
```

Appendix E

```
                line_list_concact_sort_IC4765_91171.c
/*    David Gribble, 3/6/2018

Step2
Reads in data from the concatenated file of line data and daospec
output for all selected apertures, and sorts into final Moog line list
file, in ascending order of element and ionization state, and then
wavelength. Also discards line data wavelength from input file and
keeps the corresponding daospec radial velocity corrected wavelength.
Each line is (aside from the extra wavelength value from the line data
dump) formatted for Moog input.

*/

#include <stdio.h>
#include <stdlib.h>
#include <math.h>
#include <time.h>

int main()
{
      double lambda_correct[1000], delta_lambda[1000];
      double lambda_lindat[1000], log_gf[1000], elem_ion[1000],
excit_pot_lower[1000];
      double abra, kadabra, alakazam, crucio;

      int N = 0;
      int i, j;

      FILE *in1;
      FILE *out1;

      double dummy;
      char dum;
      char buf[1000];

//can comment these three lines out if no new lines from daospec output
to add to the unsorted list
      system("cp norm_IC4765_91171.daospec foo.out");
      system("grep '#' foo.out > norm_IC4765_91171.daospec");
      system("grep '#' foo.out >> norm_IC4765_91171.daospec.main");

      /* open input & output textfiles for the data set for writing
later */
      if((in1 = fopen("norm_IC4765_91171.daospec.main", "r")) == NULL){
            printf("\nCannot open file for input\n");
      }
      if ((out1 = fopen("line_list_IC4765_91171_full_sorted.txt", "w"))
== NULL){
```

```
            printf("\nCannot open file for output\n");
      }

      while(fscanf(in1,"%lf %lf %lf %lf %lf %lf %lf %lf %lf", &abra,
&lambda_correct[N], &delta_lambda[N], &kadabra, &alakazam, &crucio,
&elem_ion[N], &excit_pot_lower[N], &log_gf[N]) != EOF){
            printf("%7.2lf   %7.3lf      %03.1lf %05.2lf %06.2lf %05.1lf
      M=%d\n", lambda_correct[N], lambda_lindat[N], elem_ion[N],
excit_pot_lower[N], log_gf[N], delta_lambda[N], N); //for debug
//          fgets(buf, 1000, in1); //for skipping to end of line for
poorly formatted/troublesome input files
            N=N+1;
            fgets(buf, 1000, in1);
      }
      fclose(in1);
      printf("file 1 scan complete N=%d\n", N);     //for debug

      fprintf(out1, "IC4765_91171, David Gribble,   03/6/18\n");

      for(i=0;i<N;i=i+1){
            for(j=i+1;j<N;j=j+1){
                  if (elem_ion[i] > elem_ion[j]){
                        dummy = elem_ion[i];
                        elem_ion[i] = elem_ion[j];
                        elem_ion[j] = dummy;

                        dummy = lambda_correct[i];
                        lambda_correct[i] = lambda_correct[j];
                        lambda_correct[j] = dummy;

                        dummy = lambda_lindat[i];
                        lambda_lindat[i] = lambda_lindat[j];
                        lambda_lindat[j] = dummy;

                        dummy = excit_pot_lower[i];
                        excit_pot_lower[i] = excit_pot_lower[j];
                        excit_pot_lower[j] = dummy;

                        dummy = log_gf[i];
                        log_gf[i] = log_gf[j];
                        log_gf[j] = dummy;

                        dummy = delta_lambda[i];
                        delta_lambda[i] = delta_lambda[j];
                        delta_lambda[j] = dummy;
                  }
                  else if ((elem_ion[i] == elem_ion[j]) &&
(lambda_correct[i] > lambda_correct[j])){
//                      if (lambda_correct[i] > lambda_correct[j]){
                              dummy = elem_ion[i];
                              elem_ion[i] = elem_ion[j];
                              elem_ion[j] = dummy;
                              //printf("elem_ion[%d]=%lf\n", i,
elem_ion[i]);    //for debug
```

```
                              dummy = lambda_correct[i];
                              lambda_correct[i] = lambda_correct[j];
                              lambda_correct[j] = dummy;

                              dummy = lambda_lindat[i];
                              lambda_lindat[i] = lambda_lindat[j];
                              lambda_lindat[j] = dummy;

                              dummy = excit_pot_lower[i];
                              excit_pot_lower[i] = excit_pot_lower[j];
                              excit_pot_lower[j] = dummy;

                              dummy = log_gf[i];
                              log_gf[i] = log_gf[j];
                              log_gf[j] = dummy;

                              dummy = delta_lambda[i];
                              delta_lambda[i] = delta_lambda[j];
                              delta_lambda[j] = dummy;
//                        }
                    }
               }
      }


            //could probably just include this within previous for loop
at end of the logic in order to save time/mem, but let's leave outside
for now to be safe
            for(i=0;i<N;i=i+1){
                  fprintf(out1, "   %6.2lf      %04.1lf    %05.2lf     %
06.2lf                         %05.1lf\n", lambda_correct[i],
elem_ion[i], excit_pot_lower[i], log_gf[i], delta_lambda[i]);
            }
/*
%[space] forces to print out '-' for negatives and a space for
positives; %0 prints leading zeros if number has less than specified
width; %# specifies total width, including before & after decimal and
the decimal itself (and I believe also includes +/- signs when they
appear); %.# specifies number of characters after the decimal
*/

      fclose(out1);

      printf("\nTask complete\n");

return(0);
}
```

Appendix F

line_list_full_sorted.txt

Solar+filt, David Gribble, 02/27/18

5622.95	06.1	08.85	-03.48	005.5
7771.96	08.0	09.15	00.32	073.7
7774.18	08.0	09.15	00.17	061.8
7775.39	08.0	09.15	-00.05	047.6
5682.64	11.0	02.10	-00.70	098.1
5688.22	11.0	02.10	-00.45	114.7
6154.23	11.0	02.10	-01.56	035.8
5528.43	12.0	04.35	-00.62	200.2
5711.10	12.0	04.35	-01.83	098.9
7387.71	12.0	05.75	-01.02	071.1
7759.37	12.0	05.93	-01.65	013.4
7811.18	12.0	05.95	-01.42	025.7
6696.04	13.0	03.14	-01.35	040.6
6698.68	13.0	03.14	-01.65	022.5
7836.12	13.0	04.02	-00.49	057.1
5645.62	14.0	04.93	-02.14	031.9
5665.56	14.0	04.92	-02.04	037.3
5684.49	14.0	04.95	-01.65	056.8
5690.44	14.0	04.93	-01.87	053.4
5708.40	14.0	04.95	-01.47	072.0
5772.15	14.0	05.08	-01.75	049.8
5793.08	14.0	04.93	-02.06	040.3
5948.54	14.0	05.08	-01.23	076.7
6091.92	14.0	05.87	-01.40	028.2
6414.99	14.0	05.87	-01.10	044.5
6555.47	14.0	05.98	-01.00	043.1
6741.64	14.0	05.98	-01.75	014.1
7405.79	14.0	05.61	-00.82	103.2
7415.95	14.0	05.62	-00.50	102.1
7760.65	14.0	06.21	-01.56	019.6
6347.09	14.1	08.12	00.30	044.9
6371.36	14.1	08.12	-00.00	029.6
6052.67	16.0	07.87	-00.74	008.8
6757.16	16.0	07.87	-00.31	013.8
5513.00	20.0	02.93	-00.29	082.4
5581.98	20.0	02.52	-00.71	089.6
5590.13	20.0	02.52	-00.71	087.0
5594.51	20.0	02.52	-00.05	151.4
5598.43	20.0	02.52	-00.22	182.8
5601.28	20.0	02.53	-00.69	103.6
6122.23	20.0	01.89	-00.41	174.5
6455.61	20.0	02.52	-01.35	056.7
6471.67	20.0	02.53	-00.59	092.8
5526.83	21.1	01.77	00.13	074.6
5657.88	21.1	01.51	-00.50	064.6
6309.89	21.1	01.50	-01.57	027.0
5460.47	22.0	00.05	-02.88	009.3

5477.72	22.0	02.43	-00.05	022.6
5490.17	22.0	01.46	-00.93	018.5
5512.51	22.0	01.46	-00.35	056.2
5514.52	22.0	01.44	-00.22	051.3
5644.09	22.0	02.27	00.03	044.0
5766.32	22.0	03.29	00.25	009.0
5866.46	22.0	01.07	-00.84	048.5
5899.31	22.0	01.05	-01.15	025.0
5965.85	22.0	01.88	-00.41	029.7
5978.55	22.0	01.87	-00.50	021.6
6126.23	22.0	01.07	-01.43	021.1
6258.69	22.0	01.46	-00.24	069.4
6261.10	22.0	01.43	-00.48	054.4
6743.14	22.0	00.90	-01.63	019.3
7489.56	22.0	02.25	-00.82	007.6
5336.80	22.1	01.58	-01.70	067.5
5418.78	22.1	01.58	-02.00	042.6
6559.59	22.1	02.05	-02.02	034.9
6606.96	22.1	02.06	-02.79	011.5
5627.63	23.0	01.08	-00.36	022.8
5670.86	23.0	01.08	-00.42	016.7
5703.60	23.0	01.05	-00.21	026.8
5727.05	23.0	01.08	-00.01	038.5
6039.73	23.0	01.06	-00.65	012.5
6090.22	23.0	01.08	-00.06	032.2
6119.54	23.0	01.06	-00.32	021.9
6150.15	23.0	00.30	-01.78	008.7
6216.36	23.0	00.28	-01.29	035.8
6243.11	23.0	00.30	-00.98	028.3
5312.85	24.0	03.45	-00.56	020.5
5329.15	24.0	02.91	-00.06	064.1
5345.81	24.0	01.00	-00.98	111.3
5348.33	24.0	01.00	-01.29	097.2
5409.80	24.0	01.03	-00.72	126.2
5442.38	24.0	03.42	-01.06	007.8
5698.38	24.0	03.88	-00.19	042.8
5702.33	24.0	03.45	-00.67	020.6
5712.78	24.0	03.01	-01.30	015.6
5783.07	24.0	03.32	-00.50	030.7
5783.87	24.0	03.32	-00.29	040.8
5787.93	24.0	03.32	-00.08	044.6
5788.39	24.0	03.01	-01.83	005.4
6330.10	24.0	00.94	-02.92	026.5
6669.30	24.0	04.18	-00.56	005.3
7400.19	24.0	02.90	-00.11	085.5
5310.68	24.1	04.07	-02.28	015.2
5313.58	24.1	04.07	-01.65	031.5
5337.75	24.1	04.07	-02.03	029.8
5510.69	24.1	03.83	-02.45	022.7
5377.62	25.0	03.84	-00.11	045.1
5394.67	25.0	00.00	-03.50	072.1
5399.49	25.0	03.85	-00.29	030.4
5407.45	25.0	02.14	-01.74	053.2
5420.37	25.0	02.14	-01.46	070.5

5470.64	25.0	02.16	-01.70	049.0
5516.79	25.0	02.18	-01.85	038.9
5537.78	25.0	02.19	-02.02	026.7
6013.50	25.0	03.07	-00.25	084.8
6016.65	25.0	03.07	-00.22	094.3
6021.80	25.0	03.08	00.03	095.6
7764.65	25.0	05.37	00.06	005.4
5315.07	26.0	04.37	-01.55	032.6
5320.04	26.0	03.64	-02.54	014.7
5321.11	26.0	04.43	-01.44	035.1
5322.05	26.0	02.28	-03.03	055.8
5324.21	26.0	03.21	-00.24	175.3
5329.99	26.0	04.08	-01.30	054.7
5332.90	26.0	01.56	-02.94	087.4
5339.94	26.0	03.27	-00.68	132.1
5358.12	26.0	03.30	-03.51	005.5
5361.62	26.0	04.42	-01.43	041.6
5369.97	26.0	04.37	00.35	136.6
5373.71	26.0	04.47	-00.86	060.0
5376.83	26.0	04.29	-02.31	012.3
5379.58	26.0	03.69	-01.48	058.8
5386.33	26.0	04.15	-01.77	030.7
5387.51	26.0	04.14	-02.14	024.1
5389.48	26.0	04.42	-00.41	080.1
5391.48	26.0	04.15	-00.82	084.1
5393.17	26.0	03.24	-00.91	127.8
5398.29	26.0	04.45	-00.67	068.0
5400.53	26.0	04.37	-00.16	116.1
5401.28	26.0	04.32	-01.92	020.0
5406.79	26.0	04.37	-01.72	030.3
5409.15	26.0	04.37	-01.30	048.0
5412.80	26.0	04.43	-01.89	014.0
5417.05	26.0	04.42	-01.53	028.4
5432.96	26.0	04.45	-01.04	067.5
5436.60	26.0	02.28	-03.39	043.0
5441.36	26.0	04.31	-01.73	029.3
5445.06	26.0	04.39	-00.02	108.3
5452.09	26.0	03.64	-02.86	011.6
5455.56	26.0	01.01	-01.75	263.5
5461.56	26.0	04.45	-01.90	022.1
5464.29	26.0	04.14	-01.72	035.9
5469.30	26.0	04.31	-02.52	005.2
5472.71	26.0	04.21	-01.72	040.0
5473.91	26.0	04.15	-00.76	076.3
5478.43	26.0	04.19	-01.85	038.8
5487.76	26.0	04.14	-00.71	089.5
5491.85	26.0	04.19	-02.40	008.2
5493.51	26.0	04.10	-01.84	036.5
5494.48	26.0	04.08	-02.09	025.4
5496.57	26.0	04.91	-01.73	006.8
5505.89	26.0	04.42	-01.38	049.1
5522.46	26.0	04.21	-01.55	041.2
5525.56	26.0	04.23	-01.33	053.2
5532.00	26.0	04.91	-01.61	013.4

5532.80	26.0	03.57	-02.15	045.7
5539.29	26.0	03.64	-02.66	015.9
5543.20	26.0	03.69	-01.57	063.5
5543.95	26.0	04.22	-01.14	061.7
5546.52	26.0	04.37	-01.31	051.4
5549.66	26.0	04.99	-01.69	008.0
5552.71	26.0	04.96	-01.99	006.0
5553.62	26.0	04.43	-01.41	055.0
5554.89	26.0	04.55	-00.44	091.5
5557.96	26.0	04.47	-01.28	059.9
5560.22	26.0	04.43	-01.19	050.6
5562.72	26.0	04.43	-00.66	061.2
5563.64	26.0	04.19	-00.99	092.8
5565.71	26.0	04.61	-00.28	085.7
5567.39	26.0	02.61	-02.80	063.2
5569.63	26.0	03.42	-00.54	142.3
5572.86	26.0	03.40	-00.31	171.5
5576.10	26.0	03.43	-01.00	108.2
5577.03	26.0	05.03	-01.55	007.7
5586.77	26.0	03.37	-00.21	177.8
5600.20	26.0	04.26	-01.81	040.2
5607.68	26.0	04.15	-02.27	011.7
5608.99	26.0	04.21	-02.40	007.7
5611.37	26.0	03.64	-02.99	006.1
5614.29	26.0	05.09	-01.52	013.3
5615.66	26.0	03.33	-00.14	211.7
5617.20	26.0	03.25	-02.88	031.0
5618.65	26.0	04.21	-01.38	048.4
5619.61	26.0	04.39	-01.70	031.6
5620.49	26.0	04.15	-01.79	036.7
5633.95	26.0	04.99	-00.27	064.5
5635.83	26.0	04.26	-01.89	032.6
5637.41	26.0	03.64	-02.50	040.4
5638.27	26.0	04.22	-00.87	074.7
5641.45	26.0	04.26	-01.18	062.5
5650.69	26.0	05.09	-00.96	034.2
5651.48	26.0	04.47	-02.00	014.8
5652.32	26.0	04.26	-01.95	023.0
5653.87	26.0	04.39	-01.64	036.3
5655.49	26.0	05.03	-00.23	067.8
5658.77	26.0	03.40	-00.92	160.0
5662.53	26.0	04.18	-00.54	089.2
5679.04	26.0	04.65	-00.92	056.3
5680.25	26.0	04.19	-02.58	006.9
5686.54	26.0	04.55	-00.63	070.1
5691.51	26.0	04.30	-01.52	036.8
5701.56	26.0	02.56	-02.22	081.9
5706.03	26.0	04.61	-00.53	084.9
5707.03	26.0	03.64	-02.40	041.0
5717.84	26.0	04.28	-01.13	062.1
5720.91	26.0	04.55	-01.95	013.5
5731.77	26.0	04.26	-01.30	058.5
5738.24	26.0	04.22	-02.34	012.8
5741.86	26.0	04.26	-01.73	031.2

5742.97	26.0	04.18	-02.51	010.7
5747.93	26.0	04.61	-01.43	037.2
5752.04	26.0	04.55	-01.27	052.8
5753.13	26.0	04.26	-00.76	077.6
5762.99	26.0	04.21	-00.45	109.6
5775.09	26.0	04.22	-01.20	057.8
5778.47	26.0	02.59	-03.59	018.9
5780.62	26.0	03.24	-02.64	042.6
5793.92	26.0	04.22	-01.70	032.8
5798.19	26.0	03.93	-01.89	043.3
5804.05	26.0	03.88	-02.29	024.9
5806.73	26.0	04.61	-01.05	053.9
5807.80	26.0	03.29	-03.41	007.5
5809.23	26.0	03.88	-01.84	049.7
5811.93	26.0	04.14	-02.43	010.2
5814.82	26.0	04.28	-01.97	022.7
5816.37	26.0	04.55	-00.68	077.8
5827.88	26.0	03.28	-03.41	010.9
5835.11	26.0	04.26	-02.37	014.0
5838.37	26.0	03.94	-02.34	019.3
5845.30	26.0	05.03	-01.82	006.2
5848.12	26.0	04.61	-00.90	039.6
5849.68	26.0	03.69	-02.99	007.2
5852.22	26.0	04.55	-01.33	040.3
5859.60	26.0	04.55	-00.40	072.6
5861.11	26.0	04.28	-02.45	006.7
5864.29	26.0	04.30	-02.52	009.0
5873.22	26.0	04.26	-02.14	016.9
5883.85	26.0	03.96	-01.36	085.8
5905.68	26.0	04.65	-00.73	050.8
5910.00	26.0	03.21	-02.78	031.4
5914.17	26.0	04.61	-00.06	130.8
5916.26	26.0	02.45	-02.99	053.9
5927.80	26.0	04.65	-01.09	040.5
5930.19	26.0	04.65	-00.23	084.8
5933.80	26.0	04.64	-02.23	006.0
5934.66	26.0	03.93	-01.17	072.8
5952.72	26.0	03.98	-01.44	058.1
5975.34	26.0	04.84	-00.82	052.5
5976.80	26.0	03.94	-01.31	073.9
5984.83	26.0	04.73	-00.34	082.5
5987.07	26.0	04.80	-00.56	074.1
6003.02	26.0	03.88	-01.12	084.2
6008.57	26.0	03.88	-01.08	088.3
6024.07	26.0	04.55	-00.12	108.2
6027.06	26.0	04.08	-01.21	066.5
6034.04	26.0	04.31	-02.42	007.5
6035.35	26.0	04.29	-02.59	005.1
6056.01	26.0	04.73	-00.46	074.4
6078.50	26.0	04.80	-00.42	077.3
6082.72	26.0	02.22	-03.57	034.6
6085.26	26.0	02.76	-03.21	042.0
6093.65	26.0	04.61	-01.50	029.5
6094.38	26.0	04.65	-01.94	017.9

6096.67	26.0	03.98	-01.93	037.3
6098.25	26.0	04.56	-01.88	014.9
6105.14	26.0	04.55	-02.05	010.3
6151.62	26.0	02.18	-03.30	051.1
6157.73	26.0	04.08	-01.26	063.7
6159.38	26.0	04.61	-01.97	010.3
6165.36	26.0	04.14	-01.55	041.3
6180.21	26.0	02.73	-02.78	058.5
6187.99	26.0	03.94	-01.72	048.3
6200.32	26.0	02.61	-02.44	074.6
6213.44	26.0	02.22	-02.66	085.1
6215.15	26.0	04.19	-01.44	067.6
6219.29	26.0	02.20	-02.43	092.3
6220.79	26.0	03.88	-02.46	018.7
6226.74	26.0	03.88	-02.22	028.9
6229.24	26.0	02.85	-02.97	038.5
6232.65	26.0	03.65	-01.27	084.9
6240.65	26.0	02.22	-03.38	049.3
6246.32	26.0	03.60	-00.96	115.1
6254.24	26.0	02.28	-02.48	116.3
6265.14	26.0	02.18	-02.55	089.7
6270.23	26.0	02.86	-02.71	056.9
6271.28	26.0	03.33	-02.95	022.9
6293.93	26.0	04.84	-01.91	010.1
6297.80	26.0	02.22	-02.74	074.3
6301.51	26.0	03.65	-00.74	113.0
6302.50	26.0	03.69	-01.20	082.5
6311.51	26.0	02.83	-03.23	026.3
6322.70	26.0	02.59	-02.43	076.5
6330.86	26.0	04.73	-01.74	031.6
6336.84	26.0	03.69	-01.05	104.7
6344.16	26.0	02.43	-02.92	064.5
6355.06	26.0	02.85	-02.42	074.6
6358.69	26.0	00.86	-04.47	085.3
6362.88	26.0	04.19	-01.97	038.0
6364.38	26.0	04.80	-01.43	028.7
6380.75	26.0	04.19	-01.40	054.5
6385.72	26.0	04.73	-01.91	011.0
6392.54	26.0	02.28	-04.03	017.8
6411.65	26.0	03.65	-00.82	129.4
6419.95	26.0	04.73	-00.24	085.6
6421.37	26.0	02.28	-02.03	115.7
6436.41	26.0	04.19	-02.46	008.1
6481.87	26.0	02.28	-02.98	065.1
6591.32	26.0	04.59	-02.07	008.8
6593.90	26.0	02.43	-02.42	092.0
6608.04	26.0	02.28	-04.03	021.5
6609.12	26.0	02.56	-02.69	075.4
6625.02	26.0	01.01	-05.35	014.2
6627.56	26.0	04.55	-01.68	026.9
6633.76	26.0	04.56	-00.78	070.6
6663.44	26.0	02.42	-02.48	098.9
6667.73	26.0	04.58	-02.15	009.3
6678.00	26.0	02.69	-01.47	134.8

6703.58	26.0	02.76	-03.16	040.8
6710.34	26.0	01.48	-04.88	016.2
6713.09	26.0	04.61	-01.51	031.2
6716.24	26.0	04.58	-01.92	017.7
6725.37	26.0	04.10	-02.30	018.2
6726.68	26.0	04.61	-00.83	051.7
6732.07	26.0	04.58	-02.21	006.4
6733.16	26.0	04.64	-01.58	028.3
6738.00	26.0	04.56	-01.75	024.0
6739.53	26.0	01.56	-04.95	012.4
6745.10	26.0	04.58	-02.16	008.6
6745.97	26.0	04.08	-02.77	006.5
6750.16	26.0	02.42	-02.62	082.0
6752.72	26.0	04.64	-01.36	038.3
7386.31	26.0	04.91	-00.40	099.5
7401.69	26.0	04.19	-01.69	043.9
7411.17	26.0	04.28	-00.43	135.2
7418.68	26.0	04.14	-01.59	057.3
7440.92	26.0	04.91	-00.68	069.4
7443.03	26.0	04.19	-01.82	041.2
7445.76	26.0	04.26	-00.24	137.2
7447.40	26.0	04.96	-01.29	035.7
7454.02	26.0	04.19	-02.41	011.7
7461.53	26.0	02.56	-03.58	031.1
7473.56	26.0	04.61	-01.87	019.5
7476.35	26.0	04.80	-01.68	020.9
7477.58	26.0	03.88	-02.90	018.7
7482.18	26.0	05.09	-01.59	017.5
7484.28	26.0	05.09	-01.70	009.1
7491.65	26.0	04.30	-01.01	071.4
7495.07	26.0	04.22	-00.10	149.3
7498.53	26.0	04.14	-02.25	017.7
7723.21	26.0	02.28	-03.62	053.3
7733.75	26.0	05.06	-01.50	013.2
7745.52	26.0	05.09	-01.29	028.4
7746.60	26.0	05.06	-01.51	025.1
7748.28	26.0	02.95	-01.76	127.9
7751.12	26.0	04.99	-00.90	060.4
7802.48	26.0	05.09	-01.58	017.5
7807.91	26.0	04.99	-00.70	065.2
7810.83	26.0	05.03	-01.27	028.9
7844.55	26.0	04.84	-01.81	013.9
5414.08	26.1	03.22	-03.79	023.4
5425.27	26.1	03.20	-03.36	036.9
5534.85	26.1	03.24	-02.93	057.4
6084.11	26.1	03.20	-03.81	019.3
6113.33	26.1	03.22	-04.16	010.3
6149.25	26.1	03.89	-02.72	035.8
6247.56	26.1	03.89	-02.33	053.2
6369.46	26.1	02.89	-04.25	017.0
6383.72	26.1	05.55	-02.27	009.4
6416.93	26.1	03.89	-02.74	042.2
6432.69	26.1	02.89	-03.71	041.4
6456.39	26.1	03.90	-02.08	062.9

7449.35	26.1	03.89	-03.31	019.5
5342.71	27.0	04.02	00.69	028.4
5352.05	27.0	03.58	00.06	021.8
5483.36	27.0	01.71	-01.49	047.9
6117.02	27.0	01.79	-02.49	006.1
6189.00	27.0	01.71	-02.45	007.6
7417.40	27.0	02.04	-02.07	009.9
5388.36	28.0	01.94	-03.56	010.3
5392.33	28.0	04.15	-01.32	011.1
5435.87	28.0	01.99	-02.59	051.6
5476.91	28.0	01.83	-00.89	145.7
5509.99	28.0	03.85	-01.29	047.3
5578.73	28.0	01.68	-02.64	053.2
5593.75	28.0	03.90	-00.84	038.4
5614.79	28.0	04.15	-00.51	041.7
5625.33	28.0	04.09	-00.70	037.7
5643.09	28.0	04.16	-01.24	012.2
5649.68	28.0	04.17	-00.81	031.0
5694.99	28.0	04.09	-00.61	039.6
5711.89	28.0	01.94	-02.27	081.9
5754.66	28.0	01.94	-02.33	074.3
5760.84	28.0	04.11	-00.80	036.3
5796.09	28.0	01.95	-03.94	007.4
5805.23	28.0	04.17	-00.64	041.1
5831.61	28.0	04.17	-01.08	025.1
5847.00	28.0	01.68	-03.21	023.5
5892.88	28.0	01.99	-02.35	076.4
5996.74	28.0	04.24	-01.06	017.3
6053.68	28.0	04.24	-01.07	020.8
6086.29	28.0	04.27	-00.53	041.7
6108.13	28.0	01.68	-02.45	066.9
6111.08	28.0	04.09	-00.87	033.9
6128.99	28.0	01.68	-03.33	025.0
6130.14	28.0	04.27	-00.96	020.3
6186.72	28.0	04.11	-00.96	030.6
6204.61	28.0	04.09	-01.13	021.4
6223.99	28.0	04.11	-00.99	027.7
6256.36	28.0	01.68	-02.48	095.4
6259.59	28.0	04.09	-01.40	019.0
6327.61	28.0	01.68	-03.15	037.5
6339.10	28.0	04.15	-00.81	046.6
6360.82	28.0	04.17	-01.28	021.9
6366.48	28.0	04.17	-01.06	026.2
6370.36	28.0	03.54	-01.94	012.0
6378.26	28.0	04.15	-00.89	032.2
6384.66	28.0	04.15	-01.13	025.2
6424.88	28.0	04.17	-01.58	014.9
6532.88	28.0	01.94	-03.39	022.9
6586.36	28.0	01.95	-02.81	050.2
6598.62	28.0	04.24	-00.98	028.3
6635.13	28.0	04.42	-00.82	024.5
6767.78	28.0	01.83	-02.17	089.2
7422.29	28.0	03.64	-00.14	111.3
7727.61	28.0	03.68	-00.17	109.9

7797.59	28.0	03.90	-00.26	084.6
5700.23	29.0	01.64	-02.31	021.5
5782.13	29.0	01.64	-01.72	072.7

Appendix G

line_list_NGC6940_full_sorted.txt

NGC6940 101, David Gribble, 02/27/18

5622.97	06.1	08.85	-03.48	020.0
7774.17	08.0	09.15	00.17	040.9
7775.41	08.0	09.15	-00.05	031.6
5682.63	11.0	02.10	-00.70	138.9
5688.22	11.0	02.10	-00.45	139.3
6154.23	11.0	02.10	-01.56	069.5
5528.43	12.0	04.35	-00.62	207.1
5711.10	12.0	04.35	-01.83	119.4
7387.68	12.0	05.75	-01.02	070.9
7759.32	12.0	05.93	-01.65	034.2
7811.12	12.0	05.95	-01.42	070.2
6696.06	13.0	03.14	-01.35	064.6
6698.68	13.0	03.14	-01.65	039.1
7836.11	13.0	04.02	-00.49	070.8
5645.61	14.0	04.93	-02.14	049.2
5684.49	14.0	04.95	-01.65	075.7
5690.43	14.0	04.93	-01.87	064.4
5772.15	14.0	05.08	-01.75	067.6
5793.08	14.0	04.93	-02.06	056.5
5948.55	14.0	05.08	-01.23	095.6
6091.90	14.0	05.87	-01.40	040.8
6414.98	14.0	05.87	-01.10	050.3
6741.62	14.0	05.98	-01.75	019.0
7405.78	14.0	05.61	-00.82	097.6
7415.95	14.0	05.62	-00.50	103.0
7760.67	14.0	06.21	-01.56	024.5
6347.09	14.1	08.12	00.30	035.8
6371.38	14.1	08.12	-00.00	023.4
6757.14	16.0	07.87	-00.31	009.8
5581.98	20.0	02.52	-00.71	115.5
5590.13	20.0	02.52	-00.71	111.0
5601.28	20.0	02.53	-00.69	142.2
6122.23	20.0	01.89	-00.41	191.2
6455.61	20.0	02.52	-01.35	088.5
6471.67	20.0	02.53	-00.59	114.6
5526.83	21.1	01.77	00.13	101.8
5657.88	21.1	01.51	-00.50	092.7
6309.85	21.1	01.50	-01.57	039.2
5460.49	22.0	00.05	-02.88	054.4
5477.71	22.0	02.43	-00.05	051.5
5490.17	22.0	01.46	-00.93	058.2
5766.33	22.0	03.29	00.25	019.8
5866.45	22.0	01.07	-00.84	106.7
5899.32	22.0	01.05	-01.15	078.6
5978.56	22.0	01.87	-00.50	062.3
6126.22	22.0	01.07	-01.43	064.6
6261.11	22.0	01.43	-00.48	100.4

6743.14	22.0	00.90	-01.63	065.6
7489.58	22.0	02.25	-00.82	035.2
5336.80	22.1	01.58	-01.70	095.1
5418.78	22.1	01.58	-02.00	073.0
6559.57	22.1	02.05	-02.02	042.9
6606.96	22.1	02.06	-02.79	024.1
5627.63	23.0	01.08	-00.36	074.5
5670.86	23.0	01.08	-00.42	068.1
5703.60	23.0	01.05	-00.21	078.9
6039.73	23.0	01.06	-00.65	049.8
6090.22	23.0	01.08	-00.06	078.1
6119.54	23.0	01.06	-00.32	066.1
6150.15	23.0	00.30	-01.78	053.2
6216.36	23.0	00.28	-01.29	086.7
6243.11	23.0	00.30	-00.98	098.4
5312.86	24.0	03.45	-00.56	037.2
5329.15	24.0	02.91	-00.06	095.9
5348.33	24.0	01.00	-01.29	138.2
5409.78	24.0	01.03	-00.72	191.4
5442.39	24.0	03.42	-01.06	020.9
5702.33	24.0	03.45	-00.67	053.0
5712.78	24.0	03.01	-01.30	041.8
5783.07	24.0	03.32	-00.50	054.5
5783.88	24.0	03.32	-00.29	074.3
5787.94	24.0	03.32	-00.08	069.3
6330.09	24.0	00.94	-02.92	061.3
7400.17	24.0	02.90	-00.11	105.4
5310.65	24.1	04.07	-02.28	018.8
5313.59	24.1	04.07	-01.65	041.4
5337.75	24.1	04.07	-02.03	050.1
5510.70	24.1	03.83	-02.45	033.7
5377.62	25.0	03.84	-00.11	076.0
5399.48	25.0	03.85	-00.29	060.1
5537.77	25.0	02.19	-02.02	094.0
6013.50	25.0	03.07	-00.25	124.3
6016.65	25.0	03.07	-00.22	129.2
6021.81	25.0	03.08	00.03	123.7
5315.07	26.0	04.37	-01.55	054.0
5321.12	26.0	04.43	-01.44	057.9
5322.06	26.0	02.28	-03.03	094.4
5324.19	26.0	03.21	-00.24	222.7
5329.96	26.0	04.08	-01.30	094.9
5332.90	26.0	01.56	-02.94	137.5
5339.94	26.0	03.27	-00.68	148.2
5358.12	26.0	03.30	-03.51	027.2
5369.97	26.0	04.37	00.35	147.4
5373.72	26.0	04.47	-00.86	078.5
5376.82	26.0	04.29	-02.31	025.8
5379.58	26.0	03.69	-01.48	084.5
5386.34	26.0	04.15	-01.77	054.0
5387.52	26.0	04.14	-02.14	054.4
5389.49	26.0	04.42	-00.41	096.3
5393.18	26.0	03.24	-00.91	147.4
5393.19	26.0	03.24	-00.91	138.9

5398.29	26.0	04.45	-00.67	079.2
5400.54	26.0	04.37	-00.16	170.0
5401.28	26.0	04.32	-01.92	043.6
5412.79	26.0	04.43	-01.89	034.3
5417.05	26.0	04.42	-01.53	049.7
5436.61	26.0	02.28	-03.39	088.9
5441.35	26.0	04.31	-01.73	050.6
5445.05	26.0	04.39	-00.02	122.7
5452.11	26.0	03.64	-02.86	036.4
5461.56	26.0	04.45	-01.90	043.8
5464.28	26.0	04.14	-01.72	062.8
5469.30	26.0	04.31	-02.52	021.8
5472.70	26.0	04.21	-01.72	065.4
5473.90	26.0	04.15	-00.76	098.8
5478.43	26.0	04.19	-01.85	066.4
5491.84	26.0	04.19	-02.40	025.3
5493.51	26.0	04.10	-01.84	068.9
5494.49	26.0	04.08	-02.09	041.7
5496.56	26.0	04.91	-01.73	020.7
5522.47	26.0	04.21	-01.55	063.5
5525.56	26.0	04.23	-01.33	077.5
5532.02	26.0	04.91	-01.61	025.5
5539.29	26.0	03.64	-02.66	040.8
5543.18	26.0	03.69	-01.57	096.0
5543.95	26.0	04.22	-01.14	086.1
5546.52	26.0	04.37	-01.31	077.7
5552.71	26.0	04.96	-01.99	015.2
5554.89	26.0	04.55	-00.44	121.8
5560.23	26.0	04.43	-01.19	072.5
5562.72	26.0	04.43	-00.66	084.1
5565.71	26.0	04.61	-00.28	105.6
5569.64	26.0	03.42	-00.54	155.7
5572.87	26.0	03.40	-00.31	190.9
5576.10	26.0	03.43	-01.00	128.8
5577.04	26.0	05.03	-01.55	017.6
5586.77	26.0	03.37	-00.21	195.3
5607.68	26.0	04.15	-02.27	028.9
5609.01	26.0	04.21	-02.40	021.3
5611.37	26.0	03.64	-02.99	018.1
5617.19	26.0	03.25	-02.88	064.6
5618.64	26.0	04.21	-01.38	070.3
5619.61	26.0	04.39	-01.70	055.7
5620.48	26.0	04.15	-01.79	073.1
5633.95	26.0	04.99	-00.27	091.8
5635.83	26.0	04.26	-01.89	053.4
5638.27	26.0	04.22	-00.87	094.1
5641.45	26.0	04.26	-01.18	091.0
5650.69	26.0	05.09	-00.96	050.2
5652.32	26.0	04.26	-01.95	042.5
5653.87	26.0	04.39	-01.64	055.5
5655.49	26.0	05.03	-00.23	081.4
5679.04	26.0	04.65	-00.92	074.5
5680.25	26.0	04.19	-02.58	024.0
5686.53	26.0	04.55	-00.63	093.0

5691.52	26.0	04.30	-01.52	061.2
5701.56	26.0	02.56	-02.22	122.1
5717.84	26.0	04.28	-01.13	083.7
5720.91	26.0	04.55	-01.95	032.7
5731.77	26.0	04.26	-01.30	083.0
5738.24	26.0	04.22	-02.34	029.9
5741.86	26.0	04.26	-01.73	055.6
5747.94	26.0	04.61	-01.43	060.8
5752.04	26.0	04.55	-01.27	069.5
5753.13	26.0	04.26	-00.76	090.7
5762.98	26.0	04.21	-00.45	142.8
5775.10	26.0	04.22	-01.20	073.8
5793.93	26.0	04.22	-01.70	055.9
5798.19	26.0	03.93	-01.89	073.8
5804.04	26.0	03.88	-02.29	058.9
5806.73	26.0	04.61	-01.05	072.5
5807.81	26.0	03.29	-03.41	026.8
5809.23	26.0	03.88	-01.84	083.0
5811.92	26.0	04.14	-02.43	025.7
5814.81	26.0	04.28	-01.97	042.4
5816.35	26.0	04.55	-00.68	113.1
5827.88	26.0	03.28	-03.41	035.1
5835.11	26.0	04.26	-02.37	032.8
5838.38	26.0	03.94	-02.34	042.7
5848.11	26.0	04.61	-00.90	069.5
5849.68	26.0	03.69	-02.99	022.2
5859.59	26.0	04.55	-00.40	089.1
5861.11	26.0	04.28	-02.45	019.8
5883.82	26.0	03.96	-01.36	099.6
5910.00	26.0	03.21	-02.78	075.1
5916.26	26.0	02.45	-02.99	093.9
5927.79	26.0	04.65	-01.09	060.4
5930.20	26.0	04.65	-00.23	113.7
5933.82	26.0	04.64	-02.23	016.0
5934.67	26.0	03.93	-01.17	099.7
5952.72	26.0	03.98	-01.44	085.4
5976.80	26.0	03.94	-01.31	105.7
5984.83	26.0	04.73	-00.34	102.4
5987.07	26.0	04.80	-00.56	090.0
6003.02	26.0	03.88	-01.12	105.5
6008.57	26.0	03.88	-01.08	109.1
6024.07	26.0	04.55	-00.12	115.5
6027.06	26.0	04.08	-01.21	090.7
6034.04	26.0	04.31	-02.42	021.5
6035.34	26.0	04.29	-02.59	015.6
6056.01	26.0	04.73	-00.46	091.1
6078.50	26.0	04.80	-00.42	092.5
6082.72	26.0	02.22	-03.57	077.5
6093.65	26.0	04.61	-01.50	049.5
6094.38	26.0	04.65	-01.94	034.9
6096.67	26.0	03.98	-01.93	062.5
6098.26	26.0	04.56	-01.88	032.6
6105.15	26.0	04.55	-02.05	022.4
6151.63	26.0	02.18	-03.30	084.1

6157.74	26.0	04.08	-01.26	090.6
6159.37	26.0	04.61	-01.97	026.2
6165.36	26.0	04.14	-01.55	065.3
6180.21	26.0	02.73	-02.78	096.8
6187.99	26.0	03.94	-01.72	071.1
6200.33	26.0	02.61	-02.44	122.2
6213.44	26.0	02.22	-02.66	124.6
6219.29	26.0	02.20	-02.43	132.1
6220.79	26.0	03.88	-02.46	043.2
6226.74	26.0	03.88	-02.22	054.4
6229.24	26.0	02.85	-02.97	075.8
6232.65	26.0	03.65	-01.27	109.0
6240.65	26.0	02.22	-03.38	087.5
6246.32	26.0	03.60	-00.96	131.8
6254.25	26.0	02.28	-02.48	150.2
6265.13	26.0	02.18	-02.55	132.6
6270.22	26.0	02.86	-02.71	091.7
6271.28	26.0	03.33	-02.95	051.3
6293.92	26.0	04.84	-01.91	021.5
6297.81	26.0	02.22	-02.74	112.8
6301.51	26.0	03.65	-00.74	131.0
6302.52	26.0	03.69	-01.20	121.4
6311.51	26.0	02.83	-03.23	063.1
6322.70	26.0	02.59	-02.43	113.0
6330.86	26.0	04.73	-01.74	050.8
6336.84	26.0	03.69	-01.05	124.9
6344.16	26.0	02.43	-02.92	109.5
6358.69	26.0	00.86	-04.47	140.4
6364.40	26.0	04.80	-01.43	058.4
6380.76	26.0	04.19	-01.40	081.6
6385.72	26.0	04.73	-01.91	022.9
6392.54	26.0	02.28	-04.03	052.7
6411.68	26.0	03.65	-00.82	119.7
6419.96	26.0	04.73	-00.24	102.5
6421.38	26.0	02.28	-02.03	163.3
6436.41	26.0	04.19	-02.46	025.1
6481.88	26.0	02.28	-02.98	103.8
6591.33	26.0	04.59	-02.07	019.5
6593.90	26.0	02.43	-02.42	127.8
6608.04	26.0	02.28	-04.03	049.8
6609.13	26.0	02.56	-02.69	112.6
6625.02	26.0	01.01	-05.35	066.6
6627.56	26.0	04.55	-01.68	048.8
6633.76	26.0	04.56	-00.78	087.5
6663.43	26.0	02.42	-02.48	141.8
6678.01	26.0	02.69	-01.47	170.3
6703.58	26.0	02.76	-03.16	075.8
6710.34	26.0	01.48	-04.88	062.1
6713.10	26.0	04.61	-01.51	058.3
6716.23	26.0	04.58	-01.92	038.5
6725.38	26.0	04.10	-02.30	036.2
6726.68	26.0	04.61	-00.83	066.9
6732.07	26.0	04.58	-02.21	015.3
6733.16	26.0	04.64	-01.58	047.0

6738.01	26.0	04.56	-01.75	044.4
6739.53	26.0	01.56	-04.95	047.2
6745.10	26.0	04.58	-02.16	016.3
6745.97	26.0	04.08	-02.77	016.0
6750.17	26.0	02.42	-02.62	117.5
6752.72	26.0	04.64	-01.36	061.0
7386.31	26.0	04.91	-00.40	108.4
7401.70	26.0	04.19	-01.69	060.9
7411.15	26.0	04.28	-00.43	126.3
7418.68	26.0	04.14	-01.59	075.2
7440.92	26.0	04.91	-00.68	078.0
7443.03	26.0	04.19	-01.82	066.1
7445.76	26.0	04.26	-00.24	142.0
7447.41	26.0	04.96	-01.29	050.3
7454.04	26.0	04.19	-02.41	029.0
7473.57	26.0	04.61	-01.87	040.5
7476.34	26.0	04.80	-01.68	036.8
7477.60	26.0	03.88	-02.90	027.8
7484.27	26.0	05.09	-01.70	016.8
7491.66	26.0	04.30	-01.01	093.4
7495.06	26.0	04.22	-00.10	154.6
7723.21	26.0	02.28	-03.62	086.8
7733.73	26.0	05.06	-01.50	024.5
7745.53	26.0	05.09	-01.29	041.0
7746.61	26.0	05.06	-01.51	036.6
7748.28	26.0	02.95	-01.76	149.2
7751.12	26.0	04.99	-00.90	071.2
7802.49	26.0	05.09	-01.58	032.8
7807.92	26.0	04.99	-00.70	084.2
7844.56	26.0	04.84	-01.81	027.2
5425.26	26.1	03.20	-03.36	051.9
5534.84	26.1	03.24	-02.93	082.0
6084.11	26.1	03.20	-03.81	036.7
6113.32	26.1	03.22	-04.16	020.8
6149.25	26.1	03.89	-02.72	047.6
6247.56	26.1	03.89	-02.33	060.3
6369.47	26.1	02.89	-04.25	031.9
6383.73	26.1	05.55	-02.27	015.1
6416.92	26.1	03.89	-02.74	051.5
6456.39	26.1	03.90	-02.08	073.5
5342.72	27.0	04.02	00.69	041.5
5352.07	27.0	03.58	00.06	040.2
6117.02	27.0	01.79	-02.49	025.8
6189.00	27.0	01.71	-02.45	040.9
7417.41	27.0	02.04	-02.07	025.8
5388.36	28.0	01.94	-03.56	039.3
5392.32	28.0	04.15	-01.32	020.4
5435.86	28.0	01.99	-02.59	085.1
5578.73	28.0	01.68	-02.64	094.1
5593.75	28.0	03.90	-00.84	056.7
5614.78	28.0	04.15	-00.51	058.8
5625.33	28.0	04.09	-00.70	055.7
5649.67	28.0	04.17	-00.81	062.1
5694.99	28.0	04.09	-00.61	056.2

5796.08	28.0	01.95	-03.94	030.9
5805.23	28.0	04.17	-00.64	058.2
5831.61	28.0	04.17	-01.08	045.7
5847.00	28.0	01.68	-03.21	063.4
5996.74	28.0	04.24	-01.06	033.1
6086.29	28.0	04.27	-00.53	061.5
6108.12	28.0	01.68	-02.45	106.7
6111.08	28.0	04.09	-00.87	053.2
6128.99	28.0	01.68	-03.33	064.4
6130.14	28.0	04.27	-00.96	034.5
6186.72	28.0	04.11	-00.96	049.8
6204.61	28.0	04.09	-01.13	043.4
6259.59	28.0	04.09	-01.40	038.1
6327.61	28.0	01.68	-03.15	081.8
6360.81	28.0	04.17	-01.28	040.8
6366.46	28.0	04.17	-01.06	061.7
6370.38	28.0	03.54	-01.94	031.8
6378.26	28.0	04.15	-00.89	051.2
6384.65	28.0	04.15	-01.13	046.0
6424.84	28.0	04.17	-01.58	027.8
6532.90	28.0	01.94	-03.39	053.9
6586.35	28.0	01.95	-02.81	095.0
6635.13	28.0	04.42	-00.82	040.1
6767.78	28.0	01.83	-02.17	120.9
7422.30	28.0	03.64	-00.14	122.9
7727.64	28.0	03.68	-00.17	125.1
7797.60	28.0	03.90	-00.26	107.7
5700.23	29.0	01.64	-02.31	076.6

Appendix H

```
                line_list_IC4765_91171_full_sorted.txt
IC4765_91171,    David Gribble,   03/15/18
   5622.97      06.1    08.85     -03.48                          026.7
   7771.95      08.0    09.15      00.32                          026.7
   7774.16      08.0    09.15      00.17                          030.2
   7775.40      08.0    09.15     -00.05                          025.2
   5682.63      11.0    02.10     -00.70                          149.4
   5688.22      11.0    02.10     -00.45                          145.8
   6154.23      11.0    02.10     -01.56                          080.6
   5528.43      12.0    04.35     -00.62                          213.6
   5711.10      12.0    04.35     -01.83                          126.3
   7387.68      12.0    05.75     -01.02                          066.6
   6696.05      13.0    03.14     -01.35                          073.9
   6698.67      13.0    03.14     -01.65                          047.3
   7836.11      13.0    04.02     -00.49                          074.7
   5645.61      14.0    04.93     -02.14                          048.4
   5690.44      14.0    04.93     -01.87                          061.2
   5772.15      14.0    05.08     -01.75                          065.3
   5793.07      14.0    04.93     -02.06                          056.9
   5948.55      14.0    05.08     -01.23                          091.5
   6414.97      14.0    05.87     -01.10                          041.6
   6741.62      14.0    05.98     -01.75                          019.8
   7405.79      14.0    05.61     -00.82                          093.2
   7415.96      14.0    05.62     -00.50                          096.6
   7760.67      14.0    06.21     -01.56                          020.9
   6347.11      14.1    08.12      00.30                          032.4
   5581.98      20.0    02.52     -00.71                          124.9
   5590.13      20.0    02.52     -00.71                          120.2
   5601.28      20.0    02.53     -00.69                          151.9
   6122.23      20.0    01.89     -00.41                          206.2
   6455.62      20.0    02.52     -01.35                          100.1
   5526.83      21.1    01.77      00.13                          107.1
   5657.88      21.1    01.51     -00.50                          098.6
   6309.90      21.1    01.50     -01.57                          039.1
   5460.50      22.0    00.05     -02.88                          082.3
   5477.72      22.0    02.43     -00.05                          064.3
   5766.34      22.0    03.29      00.25                          026.7
   5866.46      22.0    01.07     -00.84                          124.4
   5899.31      22.0    01.05     -01.15                          109.4
   5965.84      22.0    01.88     -00.41                          091.8
   5978.55      22.0    01.87     -00.50                          079.4
   6126.22      22.0    01.07     -01.43                          091.4
   6743.13      22.0    00.90     -01.63                          096.6
   7489.59      22.0    02.25     -00.82                          056.0
   5336.79      22.1    01.58     -01.70                          101.4
   5418.78      22.1    01.58     -02.00                          078.6
   6559.59      22.1    02.05     -02.02                          049.9
   6606.95      22.1    02.06     -02.79                          031.4
   5627.64      23.0    01.08     -00.36                          098.2
```

5670.86	23.0	01.08	-00.42	094.6
5703.60	23.0	01.05	-00.21	102.3
5727.05	23.0	01.08	-00.01	127.8
6039.73	23.0	01.06	-00.65	071.7
6090.22	23.0	01.08	-00.06	105.3
6119.55	23.0	01.06	-00.32	091.7
6150.16	23.0	00.30	-01.78	090.0
6216.37	23.0	00.28	-01.29	117.7
6243.10	23.0	00.30	-00.98	138.0
5312.85	24.0	03.45	-00.56	041.3
5329.15	24.0	02.91	-00.06	106.9
5345.81	24.0	01.00	-00.98	180.8
5348.33	24.0	01.00	-01.29	157.6
5409.77	24.0	01.03	-00.72	234.1
5442.38	24.0	03.42	-01.06	031.6
5712.78	24.0	03.01	-01.30	050.3
5783.08	24.0	03.32	-00.50	063.5
5783.88	24.0	03.32	-00.29	090.1
5787.94	24.0	03.32	-00.08	077.2
5788.40	24.0	03.01	-01.83	023.2
6330.10	24.0	00.94	-02.92	093.5
6669.30	24.0	04.18	-00.56	014.8
7400.18	24.0	02.90	-00.11	126.8
5310.69	24.1	04.07	-02.28	016.9
5313.60	24.1	04.07	-01.65	042.4
5337.75	24.1	04.07	-02.03	045.3
5510.69	24.1	03.83	-02.45	035.4
5377.62	25.0	03.84	-00.11	083.5
5394.67	25.0	00.00	-03.50	186.9
5394.68	25.0	00.00	-03.50	178.5
5537.77	25.0	02.19	-02.02	121.6
6013.50	25.0	03.07	-00.25	139.9
6016.65	25.0	03.07	-00.22	141.3
6021.80	25.0	03.08	00.03	140.4
5315.07	26.0	04.37	-01.55	059.1
5321.11	26.0	04.43	-01.44	061.3
5322.05	26.0	02.28	-03.03	105.2
5332.89	26.0	01.56	-02.94	164.5
5358.11	26.0	03.30	-03.51	033.4
5373.71	26.0	04.47	-00.86	083.8
5376.84	26.0	04.29	-02.31	035.7
5379.58	26.0	03.69	-01.48	093.1
5386.33	26.0	04.15	-01.77	057.1
5387.52	26.0	04.14	-02.14	061.7
5389.48	26.0	04.42	-00.41	100.4
5393.18	26.0	03.24	-00.91	161.1
5398.29	26.0	04.45	-00.67	085.2
5401.30	26.0	04.32	-01.92	048.9
5412.79	26.0	04.43	-01.89	034.2
5417.05	26.0	04.42	-01.53	051.5
5436.62	26.0	02.28	-03.39	114.6
5441.35	26.0	04.31	-01.73	054.4
5445.05	26.0	04.39	-00.02	124.5
5452.09	26.0	03.64	-02.86	036.7

5461.55	26.0	04.45	-01.90	046.0
5464.28	26.0	04.14	-01.72	068.7
5469.31	26.0	04.31	-02.52	036.1
5472.71	26.0	04.21	-01.72	070.7
5473.90	26.0	04.15	-00.76	100.9
5478.43	26.0	04.19	-01.85	066.9
5487.75	26.0	04.14	-00.71	131.1
5491.84	26.0	04.19	-02.40	027.4
5493.51	26.0	04.10	-01.84	073.9
5494.48	26.0	04.08	-02.09	056.1
5496.57	26.0	04.91	-01.73	020.3
5522.46	26.0	04.21	-01.55	063.6
5525.57	26.0	04.23	-01.33	082.2
5532.02	26.0	04.91	-01.61	030.1
5539.29	26.0	03.64	-02.66	048.5
5543.18	26.0	03.69	-01.57	100.6
5543.95	26.0	04.22	-01.14	089.0
5546.53	26.0	04.37	-01.31	085.8
5554.90	26.0	04.55	-00.44	127.3
5560.23	26.0	04.43	-01.19	076.1
5562.72	26.0	04.43	-00.66	087.3
5565.70	26.0	04.61	-00.28	113.2
5567.39	26.0	02.61	-02.80	127.4
5569.64	26.0	03.42	-00.54	164.8
5576.10	26.0	03.43	-01.00	136.1
5577.04	26.0	05.03	-01.55	016.9
5607.67	26.0	04.15	-02.27	032.8
5608.99	26.0	04.21	-02.40	028.5
5611.36	26.0	03.64	-02.99	028.9
5617.18	26.0	03.25	-02.88	058.5
5618.65	26.0	04.21	-01.38	074.6
5619.61	26.0	04.39	-01.70	059.5
5620.49	26.0	04.15	-01.79	083.0
5633.95	26.0	04.99	-00.27	081.7
5635.83	26.0	04.26	-01.89	058.4
5638.27	26.0	04.22	-00.87	100.6
5641.45	26.0	04.26	-01.18	097.4
5650.69	26.0	05.09	-00.96	051.8
5651.48	26.0	04.47	-02.00	033.3
5652.32	26.0	04.26	-01.95	047.5
5653.87	26.0	04.39	-01.64	058.4
5655.50	26.0	05.03	-00.23	085.1
5662.53	26.0	04.18	-00.54	105.7
5679.04	26.0	04.65	-00.92	077.9
5680.25	26.0	04.19	-02.58	031.3
5686.54	26.0	04.55	-00.63	097.4
5691.52	26.0	04.30	-01.52	066.2
5701.56	26.0	02.56	-02.22	133.0
5717.84	26.0	04.28	-01.13	092.9
5720.91	26.0	04.55	-01.95	034.1
5738.24	26.0	04.22	-02.34	032.1
5741.86	26.0	04.26	-01.73	058.2
5752.04	26.0	04.55	-01.27	073.6
5753.13	26.0	04.26	-00.76	098.5

5762.97	26.0	04.21	-00.45	148.5
5775.09	26.0	04.22	-01.20	084.8
5778.47	26.0	02.59	-03.59	069.5
5793.93	26.0	04.22	-01.70	061.3
5798.18	26.0	03.93	-01.89	085.8
5804.05	26.0	03.88	-02.29	067.8
5806.73	26.0	04.61	-01.05	078.6
5807.81	26.0	03.29	-03.41	035.4
5809.22	26.0	03.88	-01.84	091.4
5811.93	26.0	04.14	-02.43	028.8
5814.82	26.0	04.28	-01.97	049.1
5816.35	26.0	04.55	-00.68	120.5
5827.88	26.0	03.28	-03.41	045.3
5838.38	26.0	03.94	-02.34	050.3
5848.11	26.0	04.61	-00.90	075.9
5849.69	26.0	03.69	-02.99	031.0
5852.23	26.0	04.55	-01.33	072.5
5861.12	26.0	04.28	-02.45	016.9
5864.27	26.0	04.30	-02.52	019.1
5873.20	26.0	04.26	-02.14	044.5
5883.84	26.0	03.96	-01.36	090.2
5905.69	26.0	04.65	-00.73	074.1
5909.99	26.0	03.21	-02.78	077.3
5914.18	26.0	04.61	-00.06	158.3
5916.27	26.0	02.45	-02.99	110.0
5927.80	26.0	04.65	-01.09	062.7
5930.20	26.0	04.65	-00.23	107.9
5933.82	26.0	04.64	-02.23	014.6
5934.67	26.0	03.93	-01.17	105.9
5976.78	26.0	03.94	-01.31	101.9
5984.82	26.0	04.73	-00.34	112.2
5987.08	26.0	04.80	-00.56	096.8
6003.02	26.0	03.88	-01.12	113.7
6008.57	26.0	03.88	-01.08	116.7
6024.07	26.0	04.55	-00.12	126.8
6027.06	26.0	04.08	-01.21	097.8
6034.05	26.0	04.31	-02.42	025.1
6035.35	26.0	04.29	-02.59	017.6
6056.01	26.0	04.73	-00.46	094.3
6078.50	26.0	04.80	-00.42	096.1
6082.72	26.0	02.22	-03.57	092.6
6094.38	26.0	04.65	-01.94	036.1
6096.68	26.0	03.98	-01.93	069.1
6098.26	26.0	04.56	-01.88	038.3
6105.15	26.0	04.55	-02.05	026.5
6151.62	26.0	02.18	-03.30	106.4
6157.74	26.0	04.08	-01.26	104.7
6159.37	26.0	04.61	-01.97	030.0
6165.36	26.0	04.14	-01.55	072.9
6180.21	26.0	02.73	-02.78	107.7
6187.99	26.0	03.94	-01.72	083.2
6200.32	26.0	02.61	-02.44	127.0
6213.44	26.0	02.22	-02.66	142.7
6219.29	26.0	02.20	-02.43	150.2

6220.79	26.0	03.88	-02.46	048.5
6226.74	26.0	03.88	-02.22	056.1
6229.24	26.0	02.85	-02.97	086.0
6232.64	26.0	03.65	-01.27	118.8
6240.65	26.0	02.22	-03.38	103.2
6246.33	26.0	03.60	-00.96	138.6
6254.25	26.0	02.28	-02.48	162.6
6265.13	26.0	02.18	-02.55	155.6
6270.23	26.0	02.86	-02.71	108.3
6271.28	26.0	03.33	-02.95	059.8
6293.92	26.0	04.84	-01.91	024.3
6297.81	26.0	02.22	-02.74	132.1
6302.50	26.0	03.69	-01.20	110.8
6311.51	26.0	02.83	-03.23	072.0
6322.70	26.0	02.59	-02.43	130.5
6330.85	26.0	04.73	-01.74	046.1
6336.84	26.0	03.69	-01.05	134.7
6344.15	26.0	02.43	-02.92	126.6
6358.69	26.0	00.86	-04.47	166.8
6380.76	26.0	04.19	-01.40	089.0
6385.72	26.0	04.73	-01.91	024.2
6392.54	26.0	02.28	-04.03	066.7
6411.66	26.0	03.65	-00.82	149.1
6419.96	26.0	04.73	-00.24	106.7
6421.38	26.0	02.28	-02.03	182.5
6436.40	26.0	04.19	-02.46	028.5
6481.89	26.0	02.28	-02.98	125.9
6591.34	26.0	04.59	-02.07	025.9
6593.90	26.0	02.43	-02.42	148.8
6608.04	26.0	02.28	-04.03	071.0
6609.12	26.0	02.56	-02.69	127.5
6625.01	26.0	01.01	-05.35	101.6
6627.56	26.0	04.55	-01.68	053.6
6633.76	26.0	04.56	-00.78	091.7
6663.42	26.0	02.42	-02.48	170.7
6678.01	26.0	02.69	-01.47	192.7
6703.58	26.0	02.76	-03.16	090.1
6710.34	26.0	01.48	-04.88	089.1
6713.10	26.0	04.61	-01.51	065.7
6725.37	26.0	04.10	-02.30	042.5
6726.68	26.0	04.61	-00.83	072.1
6732.06	26.0	04.58	-02.21	017.9
6733.16	26.0	04.64	-01.58	052.6
6738.00	26.0	04.56	-01.75	051.3
6739.53	26.0	01.56	-04.95	068.5
6745.11	26.0	04.58	-02.16	020.6
6745.97	26.0	04.08	-02.77	018.5
6750.17	26.0	02.42	-02.62	137.9
6752.73	26.0	04.64	-01.36	071.8
7386.31	26.0	04.91	-00.40	111.7
7401.69	26.0	04.19	-01.69	070.7
7411.13	26.0	04.28	-00.43	151.0
7418.68	26.0	04.14	-01.59	079.9
7440.92	26.0	04.91	-00.68	083.4

7443.03	26.0	04.19	-01.82	073.3
7445.76	26.0	04.26	-00.24	156.0
7447.41	26.0	04.96	-01.29	052.6
7454.04	26.0	04.19	-02.41	037.1
7473.57	26.0	04.61	-01.87	047.4
7476.35	26.0	04.80	-01.68	037.3
7477.56	26.0	03.88	-02.90	035.8
7491.65	26.0	04.30	-01.01	093.3
7495.07	26.0	04.22	-00.10	166.3
7498.55	26.0	04.14	-02.25	044.9
7723.22	26.0	02.28	-03.62	102.1
7733.72	26.0	05.06	-01.50	022.4
7745.52	26.0	05.09	-01.29	044.1
7746.61	26.0	05.06	-01.51	039.9
7748.28	26.0	02.95	-01.76	170.0
7751.12	26.0	04.99	-00.90	077.1
7802.48	26.0	05.09	-01.58	030.0
7807.91	26.0	04.99	-00.70	086.9
7844.57	26.0	04.84	-01.81	028.2
5425.26	26.1	03.20	-03.36	047.1
5534.83	26.1	03.24	-02.93	080.9
6084.12	26.1	03.20	-03.81	033.3
6113.33	26.1	03.22	-04.16	023.8
6149.25	26.1	03.89	-02.72	042.2
6247.56	26.1	03.89	-02.33	053.0
6369.46	26.1	02.89	-04.25	026.7
6416.93	26.1	03.89	-02.74	046.6
6432.69	26.1	02.89	-03.71	054.7
6456.40	26.1	03.90	-02.08	067.1
5342.71	27.0	04.02	00.69	050.1
5352.04	27.0	03.58	00.06	056.0
6117.01	27.0	01.79	-02.49	042.6
6189.00	27.0	01.71	-02.45	067.0
7417.39	27.0	02.04	-02.07	057.4
5388.36	28.0	01.94	-03.56	051.8
5435.86	28.0	01.99	-02.59	098.1
5578.73	28.0	01.68	-02.64	109.3
5593.75	28.0	03.90	-00.84	059.8
5625.33	28.0	04.09	-00.70	057.4
5694.99	28.0	04.09	-00.61	057.7
5754.66	28.0	01.94	-02.33	132.6
5760.84	28.0	04.11	-00.80	055.1
5796.08	28.0	01.95	-03.94	042.0
5805.23	28.0	04.17	-00.64	056.9
5831.61	28.0	04.17	-01.08	047.8
5847.00	28.0	01.68	-03.21	080.1
5996.73	28.0	04.24	-01.06	035.0
6053.67	28.0	04.24	-01.07	040.5
6086.29	28.0	04.27	-00.53	061.3
6108.12	28.0	01.68	-02.45	123.1
6111.08	28.0	04.09	-00.87	055.4
6128.99	28.0	01.68	-03.33	081.9
6130.14	28.0	04.27	-00.96	035.2
6186.72	28.0	04.11	-00.96	051.7

6204.61	28.0	04.09	-01.13	045.6
6259.58	28.0	04.09	-01.40	040.5
6327.61	28.0	01.68	-03.15	100.4
6360.80	28.0	04.17	-01.28	041.9
6370.39	28.0	03.54	-01.94	039.0
6378.26	28.0	04.15	-00.89	054.0
6384.64	28.0	04.15	-01.13	048.4
6424.84	28.0	04.17	-01.58	026.6
6532.90	28.0	01.94	-03.39	071.1
6586.33	28.0	01.95	-02.81	097.1
6635.12	28.0	04.42	-00.82	043.5
6767.78	28.0	01.83	-02.17	142.3
7422.31	28.0	03.64	-00.14	133.1
7727.62	28.0	03.68	-00.17	123.3
7797.59	28.0	03.90	-00.26	110.1
5700.23	29.0	01.64	-02.31	105.8
5782.12	29.0	01.64	-01.72	164.7

Appendix I

```
                          model.NGC_6940101
BEGN
teff= 5132. grav= 3.13 abund= 0.10 turb= 1.46
             34       (6e13.4)
   0.1000E-03   0.3737E+04   0.2308E+01  -0.1874E+01   0.1299E+01
0.1222E-02
   0.2000E-03   0.3794E+04   0.2415E+01  -0.1750E+01   0.1299E+01
0.1552E-02
   0.3000E-03   0.3847E+04   0.2521E+01  -0.1632E+01   0.1299E+01
0.1946E-02
   0.4000E-03   0.3897E+04   0.2626E+01  -0.1518E+01   0.1299E+01
0.2425E-02
   0.6000E-03   0.3946E+04   0.2731E+01  -0.1405E+01   0.1299E+01
0.3012E-02
   0.1000E-02   0.3993E+04   0.2836E+01  -0.1293E+01   0.1299E+01
0.3735E-02
   0.1600E-02   0.4040E+04   0.2942E+01  -0.1183E+01   0.1299E+01
0.4612E-02
   0.2500E-02   0.4085E+04   0.3048E+01  -0.1073E+01   0.1299E+01
0.5687E-02
   0.4000E-02   0.4127E+04   0.3155E+01  -0.9656E+00   0.1299E+01
0.7006E-02
   0.6300E-02   0.4167E+04   0.3263E+01  -0.8589E+00   0.1299E+01
0.8628E-02
   0.1000E-01   0.4207E+04   0.3371E+01  -0.7522E+00   0.1300E+01
0.1063E-01
   0.1580E-01   0.4250E+04   0.3479E+01  -0.6439E+00   0.1300E+01
0.1313E-01
   0.2510E-01   0.4300E+04   0.3587E+01  -0.5328E+00   0.1300E+01
0.1626E-01
   0.3980E-01   0.4360E+04   0.3694E+01  -0.4177E+00   0.1300E+01
0.2019E-01
   0.6310E-01   0.4433E+04   0.3802E+01  -0.2973E+00   0.1300E+01
0.2516E-01
   0.1000E+00   0.4524E+04   0.3908E+01  -0.1708E+00   0.1300E+01
0.3139E-01
   0.1585E+00   0.4640E+04   0.4014E+01  -0.3720E-01   0.1300E+01
0.3904E-01
   0.2512E+00   0.4791E+04   0.4120E+01   0.1055E+00   0.1300E+01
0.4841E-01
   0.3162E+00   0.4880E+04   0.4173E+01   0.1798E+00   0.1299E+01
0.5382E-01
   0.3981E+00   0.4983E+04   0.4227E+01   0.2585E+00   0.1299E+01
0.5992E-01
   0.5012E+00   0.5100E+04   0.4280E+01   0.3434E+00   0.1299E+01
0.6709E-01
   0.6310E+00   0.5234E+04   0.4332E+01   0.4394E+00   0.1299E+01
0.7639E-01
```

```
   0.7943E+00   0.5385E+04   0.4383E+01   0.5537E+00   0.1299E+01
0.8999E-01
   0.1000E+01   0.5556E+04   0.4430E+01   0.6940E+00   0.1299E+01
0.1117E+00
   0.1259E+01   0.5746E+04   0.4472E+01   0.8637E+00   0.1299E+01
0.1472E+00
   0.1585E+01   0.5960E+04   0.4507E+01   0.1062E+01   0.1299E+01
0.2051E+00
   0.1995E+01   0.6198E+04   0.4536E+01   0.1283E+01   0.1299E+01
0.3037E+00
   0.2512E+01   0.6463E+04   0.4559E+01   0.1521E+01   0.1298E+01
0.4660E+00
   0.3162E+01   0.6759E+04   0.4577E+01   0.1772E+01   0.1297E+01
0.7355E+00
   0.3981E+01   0.7097E+04   0.4590E+01   0.2037E+01   0.1296E+01
0.1210E+01
   0.5012E+01   0.7445E+04   0.4600E+01   0.2287E+01   0.1293E+01
0.2013E+01
   0.6310E+01   0.7730E+04   0.4608E+01   0.2478E+01   0.1290E+01
0.3016E+01
   0.7943E+01   0.7956E+04   0.4615E+01   0.2621E+01   0.1286E+01
0.4106E+01
   0.1000E+02   0.8142E+04   0.4621E+01   0.2732E+01   0.1282E+01
0.5273E+01
    0.146E+01
NATOMS        0     0.10
NMOL         16
     101.0     106.0     107.0     108.0     606.0     607.0     608.0
707.0
     708.0     808.0   10108.0   60808.0     112.0     812.0     822.0
814.0
```

Appendix J

```
                          model.IC4765_91171
BEGN
teff= 4739. grav= 2.48 abund= 0.10 turb= 1.58
             34       (6e13.4)
   0.1000E-03   0.3418E+04   0.2089E+01  -0.2341E+01   0.1300E+01
0.4755E-03
   0.2000E-03   0.3480E+04   0.2189E+01  -0.2201E+01   0.1300E+01
0.6384E-03
   0.3000E-03   0.3533E+04   0.2285E+01  -0.2077E+01   0.1300E+01
0.8259E-03
   0.4000E-03   0.3581E+04   0.2381E+01  -0.1960E+01   0.1300E+01
0.1048E-02
   0.6000E-03   0.3627E+04   0.2477E+01  -0.1847E+01   0.1300E+01
0.1317E-02
   0.1000E-02   0.3670E+04   0.2574E+01  -0.1737E+01   0.1300E+01
0.1647E-02
   0.1600E-02   0.3714E+04   0.2672E+01  -0.1627E+01   0.1300E+01
0.2054E-02
   0.2500E-02   0.3756E+04   0.2772E+01  -0.1517E+01   0.1300E+01
0.2557E-02
   0.4000E-02   0.3799E+04   0.2873E+01  -0.1408E+01   0.1300E+01
0.3180E-02
   0.6300E-02   0.3842E+04   0.2975E+01  -0.1298E+01   0.1300E+01
0.3955E-02
   0.1000E-01   0.3887E+04   0.3077E+01  -0.1188E+01   0.1300E+01
0.4924E-02
   0.1580E-01   0.3934E+04   0.3180E+01  -0.1076E+01   0.1300E+01
0.6142E-02
   0.2510E-01   0.3986E+04   0.3283E+01  -0.9610E+00   0.1300E+01
0.7687E-02
   0.3980E-01   0.4046E+04   0.3386E+01  -0.8420E+00   0.1300E+01
0.9643E-02
   0.6310E-01   0.4118E+04   0.3488E+01  -0.7168E+00   0.1300E+01
0.1216E-01
   0.1000E+00   0.4206E+04   0.3589E+01  -0.5841E+00   0.1300E+01
0.1543E-01
   0.1585E+00   0.4318E+04   0.3689E+01  -0.4434E+00   0.1300E+01
0.1962E-01
   0.2512E+00   0.4461E+04   0.3789E+01  -0.2943E+00   0.1300E+01
0.2483E-01
   0.3162E+00   0.4545E+04   0.3839E+01  -0.2184E+00   0.1300E+01
0.2776E-01
   0.3981E+00   0.4641E+04   0.3889E+01  -0.1406E+00   0.1299E+01
0.3087E-01
   0.5012E+00   0.4749E+04   0.3939E+01  -0.6110E-01   0.1299E+01
0.3417E-01
   0.6310E+00   0.4872E+04   0.3991E+01   0.2130E-01   0.1299E+01
0.3777E-01
```

```
   0.7943E+00   0.5010E+04   0.4042E+01   0.1104E+00   0.1299E+01
0.4207E-01
   0.1000E+01   0.5166E+04   0.4093E+01   0.2143E+00   0.1299E+01
0.4813E-01
   0.1259E+01   0.5340E+04   0.4142E+01   0.3451E+00   0.1299E+01
0.5813E-01
   0.1585E+01   0.5536E+04   0.4186E+01   0.5117E+00   0.1299E+01
0.7568E-01
   0.1995E+01   0.5753E+04   0.4224E+01   0.7141E+00   0.1299E+01
0.1063E+00
   0.2512E+01   0.5994E+04   0.4254E+01   0.9449E+00   0.1299E+01
0.1581E+00
   0.3162E+01   0.6260E+04   0.4278E+01   0.1196E+01   0.1298E+01
0.2499E+00
   0.3981E+01   0.6555E+04   0.4295E+01   0.1459E+01   0.1297E+01
0.4067E+00
   0.5012E+01   0.6885E+04   0.4308E+01   0.1731E+01   0.1296E+01
0.6805E+00
   0.6310E+01   0.7239E+04   0.4318E+01   0.2000E+01   0.1293E+01
0.1164E+01
   0.7943E+01   0.7542E+04   0.4325E+01   0.2212E+01   0.1289E+01
0.1837E+01
   0.1000E+02   0.7772E+04   0.4330E+01   0.2363E+01   0.1285E+01
0.2579E+01
    0.158E+01
NATOMS        0     0.10
NMOL         16
     101.0     106.0     107.0     108.0     606.0     607.0     608.0
707.0
     708.0     808.0   10108.0   60808.0     112.0     812.0     822.0
814.0
```

Vita

David Gribble was born in Oakland, California, to Chip and Linda Gribble, joining his older brother, Stephen. He grew up in Richmond, California, and attended El Cerrito High School in the neighboring town of El Cerrito. He enrolled at the University of California, Davis, in 2008, where he completed a Bachelor of Science degree in Physics, with an emphasis in Astrophysics, as well as two minors in Geophysics and African-American Studies, in 2014. During his time at UC Davis, he conducted research with Dr. Thomas Cahill in the fields of applied nuclear science and environmental physics and also interned for a period at the Federation of American Scientists, under Dr. Charles Ferguson.

After graduating from UC Davis, he taught environmental education and middle-school science at Caritas Creek in Occidental, California, and even had a brief tenure as a stand-up comedian. In 2016, he returned to academia and enrolled in the Master of Science program in Engineering Physics at Appalachian State University in Boone, NC. He received the M.S. in August 2018. In the Fall of 2018 he will begin study in the Ph.D. program in Physics at the University of North Carolina, Chapel Hill, where he is excited to work with the Nuclear Astrophysics group.